Preparation of the JTT mixture culture medium

JTT extract powder was dissolved in Dulbecco's Modified Eagle's Medium (DMEM, Sigma) by stirring at room temperature for 1 hr at a concentration of 2 mg/ml. After dissolved, it was sonicated for 30 min (Branson Sonifier 250, Danbury, CT, USA), and centrifuged at 3,000 rpm for 10 min (J6-HC Centrifuge, Beckman Coulter, Fullerton, CA, USA) to remove the insoluble materials. The supernatant was then filtered with a disposable syringe filter with a 0.22 μm PVDF membrane (Millipore, Cork, Ireland). This solution was then added with 10% fetal bovine serum (FBS, ICN Biomedicals, Aurora, OH, USA), 0.2% glucose and 5 μg/ml bovine insulin to prepare the JTT mixture culture medium.

Preparation and culture of primary microglia and Ra2 cell lines

Mouse primary microglia were isolated from primary mixed glial cell cultures obtained from newborn C57BL/6 mice by the "shaking off" method as described previously (Suzumura et al. 1987). In brief, after the meninges were carefully removed under microscope, the brains were dissociated by passing it through a 258-μm-pore nylon mesh. The cell suspension was washed twice with Hank's balanced salt solution, triturated and placed in 75-cm^2 culture flasks at a density equivalent of two brains per flask in 10 ml DMEM supplemented with 10% FBS, 0.2% glucose and 5 μg/ml bovine insulin. On the 14th day, the mixed glial cell cultures were put into Bio Shaker (TAITEC, BR-43FM, Koshigaya), and were shaken at 37°C, 150 rpm for 3 hrs. The medium was collected, centrifuged, and the harvested cells were incubated at 37°C, 5% CO_2 for 30 min. The attached cells were harvested by cell scraper. The morphological change was observed under an Olympus IX70 microscope (Olympus, Tokyo) and recorded with a Nikon digital camera DXM1200F (Nikon, Tokyo). The purity of cultured microglia was 97-100% as determined by indirect immunofluorescence staining with antibody to Iba1.

The microglial cell line Ra2 cells established from neonatal C57BL/6J (H-2^b) mice using a non-enzymatic and non-virus-transformed procedure (Sawada et al. 1998) were kindly provided by Dr. Sawada (Department of Brain Function, Research Institute of Environmental Medicine, Nagoya University, Nagoya). Ra2 cells proliferated in the same culture medium as primary microglia supplemented with 1 ng/ml GM-CSF. Before experiment, the Ra2 cells were cultured without GM-CSF for 16 hrs.

Preparation and culture of bone marrow-derived macrophages (BMM)

12-week-old female C57BL/6 wild type mice were used in this experiment. This experiment was performed under the guidelines for Animal Experiments of National Center for Geriatrics and Gerontology and approval of the institute's ethical committee for animal experiment. 8 mice were randomly divided into two groups. One group (experimental group, n = 4) was given drinking water containing 100 mg/ml of JTT. The dose was determined according to our previous study (Hara et al. unpublished). The drinking water was prepared by the similar protocol with the preparation of JTT mixture culture medium mentioned above. Since 20% of JTT was removed by the procedure of sedimentation during the preparation and each animal consumed 3 ml of the drinking water per day, the average consumption of JTT was estimated as 250 mg/day/caput. If animals spill over about 20% of drinking water, this is about 100 times higher than the dosage for human use. The other group (control group, n = 4) was given plain drinking water. After 21 days, isolation of BMM was performed by a modified method published by Takahashi and collaborators (Takahashi et al. 2007). In detail, the mice were sacrificed by decapitation and bone marrow cells were freshly flushed from the medullary cavities of the femurs and tibias with a 25 ga needle, and then filtered through a 40 μm nylon mesh. Removal of erythrocytes was performed by lysis with hypotonic solution, followed by washing twice with Dulbecco's PBS containing 2% FBS. The cells were then resuspended in DMEM containing 10% FBS and 10 ng/ml M-CSF in 75-cm^2 culture flasks. After 24 hrs, non-adherent cells were collected and re-seeded in fresh 75-cm^2 culture flasks. Medium was changed every three days, and BMM were collected for f$A\beta_{42}$-phagocytosis assay after 12 - 13 days. The purity of BMM was more than 95% as determined by indirect immunofluorescence staining with antibody to Iba1.

Cell proliferation (WST-1) assay

Primary microglia at a density of 2 × 10^4 cells/well were plated onto a 96-well microtiter plate. Different concentrations of JTT (10, 50, 100, 200, 400 and 600 μg/ml) or LPS (0.1 μg/ml) as positive control were added to the culture medium for 48 hrs. Cell proliferation assay was determined by the PreMix WST-1 cell proliferation assay system (TaKaRa, Tokyo). This assay bases on the cleavage of tetrazolium salts which were added into the medium. These teterazolium salts are cleaved to forma-

zan dye by succinate-tetrazolium reductase, which exists in the mitochondrial respiratory chain and is active only in viable cells. At the end of the experiments, 10 μl/well PreMix WST-1 reagent was added followed by incubating at 37°C, 5% CO_2 for 4 hrs. The absorbance at the wavelength of 450 nm was measured by a microplate reader (model 550, Bio-Rad Laboratories, Hercules, CA, USA).

Flow cytometric assay

Ra2 cells were treated with different concentrations of JTT (200 and 400 μg/ml) or LPS (0.1 μg/ml) for 48 hrs. The cells were detached and single cell suspensions were made in fluorescence activated cell sorting (FACS) buffer consisting of Dulbecco's PBS containing 4% FBS and 0.1% sodium azide. The cells were then incubated with FITC-conjugated rat anti-mouse CD11b monoclonal antibody for cell surface staining at 4°C for 30 min. After washed twice with FACS buffer to remove the antibody completely, the samples were examined by FACSCalibur flow cytometer (BD, Franklin Lakes, NJ, USA) and analyzed using the Cellquest™ software (BD immunocytometry system, CA, USA).

Immunofluorescence staining for fAβ_{42}-phagocytosis assay

Both primary microglia in vitro pre-treated with different concentrations of JTT (100, 200, 400 or 600 μg/ml) for 24 hrs or pre-treated with 200 μg/ml JTT for different time periods (12, 24 or 48 hrs) and BMM from two groups which were in vivo pre-administrated with or without 100 mg/ml JTT were used for fAβ_{42}-phagocytosis assay. At the end of each treatment, the culture medium was changed and fAβ_{42} was added to a final concentration of 1 μM, followed by incubation for further 3 hrs. After fixation with 4% paraformaldehyde at 4°C for 15 min, the cells were blocked and permeabilized with PBS containing 5% normal donkey serum, 0.5% bovine serum albumin and 0.2% Triton X-100 at room temperature for 1 h. Microglia or BMM were then stained with anti-Iba1 antibody (1 : 250) or anti-LAMP-2 antibody (1:250), and fAβ_{42} was stained with 4G8 antibody (1:500) at 4°C overnight. After 3-time washes with PBS, specific binding was detected using secondary antibodies: Alexa 488-conjugated donkey anti-rabbit IgG and Alexa 594-conjugated donkey anti-mouse IgG (Molecular Probes, Eugene, OR, USA). After washing, the fluorescence was observed by an Olympus IX70 microscope equipped with appropriate filters. The fAβ_{42}-phagocytosed microglia in each group were counted in at least three randomly chosen areas containing more than 200 Iba1 or LAMP-2 positive cells under fluorescence microscope as the total cell numbers. When stained with anti-Iba1 antibody, the numbers of microglia containing engulfed fAβ_{42} were determined by counting cells with Alexa 594 internalization around nuclei other than on the cell surface. When stained with anti-LAMP-2 antibody, the numbers of microglia containing engulfed fAβ_{42} were determined by counting cells with the colocalization of Alexa 488 and Alexa 594 fluorescence. The percentages of fAβ_{42}-phagocytosed microglia pre-treated with different concentrations of JTT were shown as means and standard deviation (S.D.) from three independent experiments with Iba1 and 4G8 staining and one experiment with LAMP-2 and 4G8 staining. While the percentages of fAβ_{42}-phagocytosed microglia pre-treated with 200 μg/ml JTT for different time periods were shown as means and SD from three independent experiments with Iba1 and 4G8 staining. The percentages of fAβ_{42}-phagocytosed BMM were analyzed similarly from four mice per group with Iba1 and 4G8 staining.

Nitric oxide (NO) quantification

The Griess reaction is extensively used as an indicator of NO production by cultured cells. Primary microglia were plated on 48-well culture plates at 1×10^5 cells/well, and treated with or without 200 μg/ml JTT for 24 hrs. Afterwards, the culture medium was changed with or without 10 μM fAβ_{42} for another 24 hrs incubation. The media collected were centrifuged and the cell-free supernatants were then quantitatively determined for total NO production using a total NO assay kit (Endogen, Pierce Biotechnology, Rockford, IL, USA). The assay was carried out according to the manufacturer's protocol.

Statistical analyses

All results were expressed as means ± S.D. The statistical significance of differences was determined by two-tailed Student's *t*-test or analysis of variance (ANOVA) followed by the post-hoc multiple comparison.

Results

Effects of JTT on the morphological change of microglial activation

The effect of JTT on microglial activation was first revealed by observing prominent morphological changes of primary microglia treated with JTT under the phase contrast microscope. It

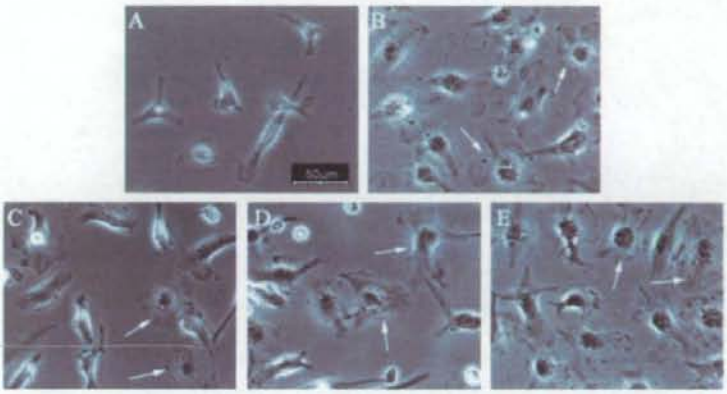

Fig. 1. JTT changed the morphological appearance of primary microglia. Primary microglia were cultured for 24 hrs in (A) unstimulated condition, (B) LPS (0.1 μg/ml), (C) JTT (100 μg/ml), (D) JTT (200 μg/ml), and (E) JTT (400 μg/ml) and observed under the phase contrast microscope. The arrows show some of the activated microglia with amoeboid morphology. Scale bar, 50 μm.

is well known that resting microglia adopt a characteristic highly ramified and elongated morphological appearance with small cell bodies, while activated microglia undergo dramatic morphological changes showing amoeboid morphology with large cell bodies and short processes (Kreutzberg 1996). When we treated primary microglia with different concentrations of JTT or LPS for 24 hrs, we observed that they showed obvious activated morphological appearance, particularly in 200 and 400 μg/ml JTT-treated groups (Fig. 1).

Effect of JTT on microglial proliferation and viability

To investigate the possible role of JTT in the proliferation and activation of microglia, next we examined whether JTT could sustain the cell proliferation of primary microglia by the WST-1 assay. As expected, JTT increased microglial proliferation and viability in a slightly dose-dependent fashion. Compared with LPS, JTT showed similar or more promoting effects on microglial proliferation and viability (Fig. 2). From this result and the above morphological change result, we chose the concentrations of 200 and 400 μg/ml for some of the following experiments.

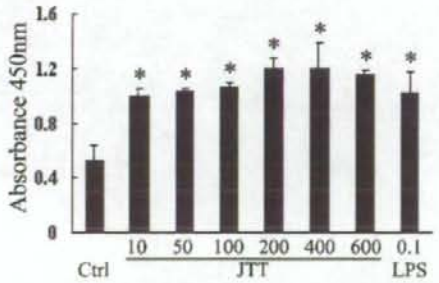

Fig. 2. JTT induced cell proliferation of primary microglia by the WST-1 cell proliferation assay. Primary microglia were seeded at a density of 2×10^4 cells/well in a 96-well microtiter plate as described in the Materials and Methods. After treatment with different concentrations of JTT as well as LPS as a positive control for 48 hrs, the cultures were added with the WST-1 reagent followed by 4 hrs incubation, and then the absorbance at 450 nm was measured. Mean ± S.D. values from a single experiment were obtained in triplicate. Similar results were obtained in two separate experiments. $^*p < 0.01$ vs control group (unstimulated condition) analyzed by Dunnett's test in ANOVA.

Effect of JTT on the surface expression of CD11b

The flow cytometric assay was used to check the expression of surface marker CD11b on microglial cell line Ra2, which indicates the activation of microglia. Ra2 cells have been confirmed to have similar properties to primary microglia, and have been generally used as the substitutes of primary microglia in experimental research (Ito et al. 2005, 2006; Laquintana et al. 2007; Roepstorff et al. 2007). Ra2 cells were used in the flow cytometric assay because they showed easily-detached property after treatment than primary microglia. So Ra2 cells were more suitable for this assay in order to obtain more creditable results. Two peaks were obtained apparently in every treated group but not in an unstimulated condition after either 24 or 48 hrs treatment, indicating that the latter peak should be formed by activated cells (M1). After 24 hrs treatment with JTT or LPS, the percentage of activated cell number and their mean fluorescence intensity (mFI) were both increased compared to the negative control group, but there was no significant difference (data not shown). However, after 48 hrs treatment, there was significant difference when the above two indexes were analyzed, while there was no difference between the 200 and 400 μg/ml JTT treatment groups (Fig. 3). JTT increased the cell number percentage and mFI of M1 by about 50% and 170%, respectively, relative to the negative control. These results

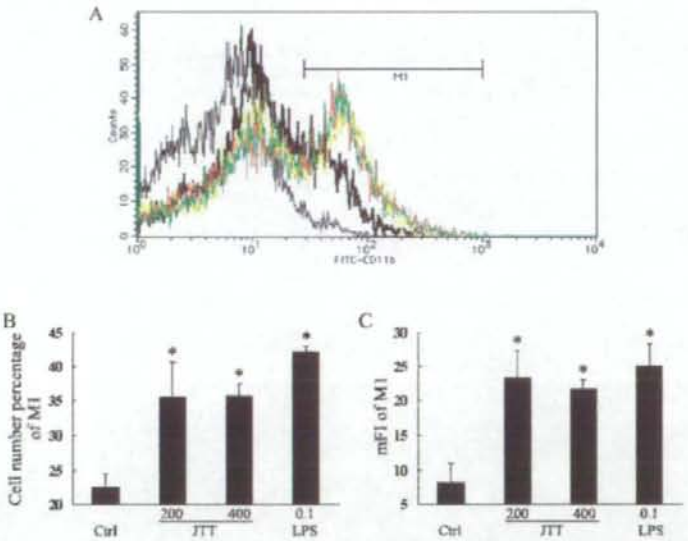

Fig. 3. JTT increased the surface expression of CD11b. Ra2 microglial cells were treated with 200, 400 μg/ml JTT or 0.1 μg/ml LPS for 48 hrs as described in the Materials and Methods. After gently detached, Ra2 cells were stained with FITC-conjugated anti-CD11b antibody for the FACS analysis. (A) Overlay of flow cytometry histograms of untreated cells without staining (gray line), untreated cells as control (black line), 200 μg/ml JTT-treated cells (red line), 400 μg/ml JTT-treated cells (yellow line) and LPS-treated cells (green line). M1, which referred to the second peak, represents the activated cells whose CD11b expression was increased. (B) The cell number percentage of M1 in each group. (C) Mean fluorescence intensity of M1 in each group. Mean ± S.D. values from a single experiment were performed in triplicate. Similar results were obtained in two independent experiments. $^{*}p < 0.01$ vs control group analyzed by Dunnett's test in ANOVA.

confirmed that JTT could induce the surface expression of an activation marker CD11b on microglia, but it might take at least 48 hrs to show this effect.

Effect of JTT on Microglial Phagocytosis of fAβ_{42}

Since the above findings confirmed that JTT could induce the proliferation and activation of microglia, we next examined whether JTT could enhance microglial phagocytosis of fAβ_{42}. We could see that JTT did enhance the microglial phagocytosis of fAβ_{42} obviously after 24 hrs treatment when the concentration of JTT was higher than 200 μg/ml, but did not show a concentration-dependent fashion (Fig. 4E). The 200 μg/ml JTT-treated group got the highest percentage of phagocytosed cells of 60.5 ± 5.4%, which is higher than the negative control (33.7 ± 4.4%) and the LPS positive control (46.9 ± 2.3%) by 26.8 ± 1.3% and 13.6 ± 6.2%, respectively. To examine whether the effect of JTT showed time-dependent fashion, 200 μg/ml JTT was used to treat primary microglia for different time periods. The 24 hrs treatment group showed the highest percentage of phagocytosed cells of 60.4 ± 4.4%. No evident time-dependent fashion was seen as shown in Fig. 4F.

Effect of JTT on BMM phagocytosis of fAβ_{42}

The fAβ_{42} phagocytosis was also investigated in BMM in this study. The BMM from the two groups (four mice each) which had been pre-administrated with or without JTT were cultured for 12 - 13 days as described above, and then their ability of fAβ_{42} phagocytosis was examined using

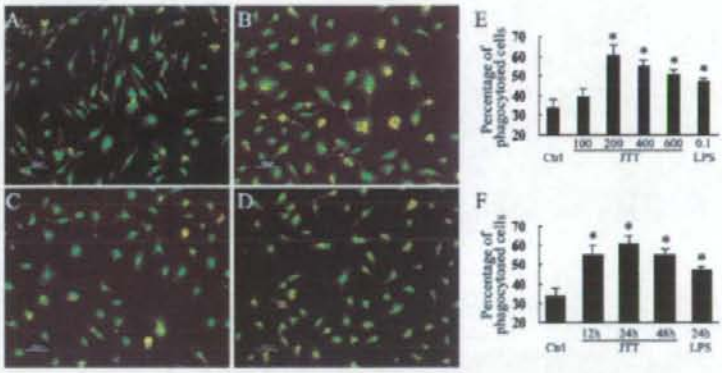

Fig. 4. JTT enhanced the phagocytosis of fAβ_{42} in primary microglia. Primary microglia were treated with JTT or LPS. Then the culture medium was changed and 1 μM fAβ_{42} was added for further 3 hrs incubation followed by immunofluorescence double staining as described in the Materials and Methods. (A-D) The cells were stained with antibodies directed against Iba1 and 4G8, and then with Alexa 488 (green) and Alexa 594 (red)-conjugated secondary antibodies, respectively. Under fluorescence microscope, colocalization of microglia and fAβ_{42} was shown by yellow color as a result of superimposing fluorescence images of microglia (green) and fAβ_{42} (red). (A) Control (unstimulated condition, 24 hrs). (B) JTT (200 μg/ml, 24 hrs). (C) JTT (400 μg/ml, 24 hrs). (D) LPS (0.1 μg/ml, 24 hrs). (E) Microglia were treated with different concentrations of JTT or LPS for 24 hrs. Percentages of phagocytosed cells were counted. Mean ± S.D. values were obtained from three separate experiments with Iba1 and 4G8 staining and one experiment with LAMP-2 and 4G8 staining (figure not shown). (F) Microglia were treated with 200 μg/ml JTT for distinct time periods (12, 24, 48 hrs) or 0.1 μg/ml LPS for 24 hrs. Percentages of phagocytosed cells were counted (figure not shown). Mean ± S.D. values were obtained from three separate experiments with Iba1 and 4G8 staining. Scale bars represent 50 μm. *$p < 0.01$ vs control group analyzed by Dunnett's test in ANOVA.

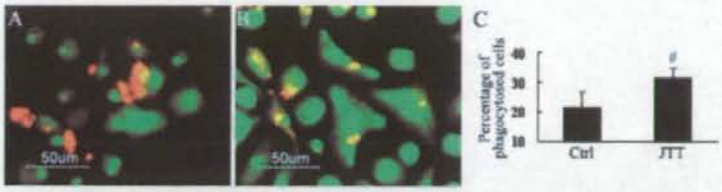

Fig. 5. JTT enhanced the phagocytosis of fAβ_{42} in BMM. BMM were obtained from mice with or without JTT administration and cultured for about 2 weeks. Then the culture medium was changed and 1 μM fAβ_{42} was added for further 3 hrs incubation followed by immunofluorescence double staining as described in the Materials and Methods. (A-B) The cells were stained with antibodies directed against Iba1 and 4G8, and then with Alexa 488 (green) and Alexa 594 (red)-conjugated secondary antibodies, respectively. Under fluorescence microscope, colocalization of BMM and fAβ_{42} was shown by yellow color as a result of superimposing fluorescence images of BMM (green) and fAβ_{42} (red). (A) Control group (without JTT administration), (B) JTT administration group, (C) Percentages of phagocytosed cells. Mean ± S.D. values were obtained from four mice. Scale bars represent 50 μm. #$p < 0.05$ vs control group analyzed by two-tailed Student's t test.

immunofluorescence double staining according to the same protocol mentioned above. As shown in Fig. 5, some BMM from JTT-administrated mice showed larger cell bodies and stronger signal of Iba1 staining (Fig. 5B) compared to the control group (Fig. 5A), as well as the higher percentage of fAβ_{42}-phagocytosed cells (31.6 ± 3.3% vs 21.6 ± 5.2%, respectively, $p < 0.05$) (Fig. 5C).

Effect of JTT on NO production in primary microglia

The effect of JTT treatment on NO production in primary microglia was investigated by the Griess reaction. The ratio of NO production to the control group was shown in Fig. 6. Twenty hundred μg/ml JTT was used to treat primary microglia. It slightly increased NO production but no statistical difference compared to the control group ($p = 0.396$), but LPS or 10 μM fAβ_{42} did increase ($p = 0.000$ and 0.008, respectively). And between the JTT and LPS groups, there was also significant difference ($p = 0.002$). In the presence of 10 μM fAβ_{42}, although JTT treatment did not reduce the NO production, at least it did not increase the NO production ($p = 0.396$).

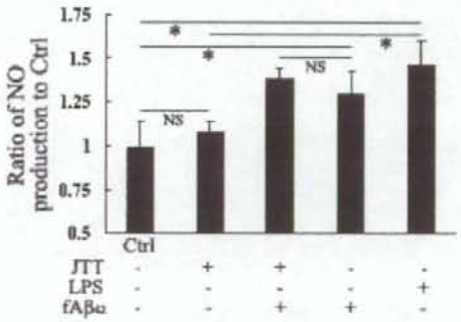

Fig. 6. JTT did not increase the production of NO in primary microglia. Primary microglia were treated with 200 μg/ml JTT or 0.1 μg/ml LPS for the first 24 hrs, then the culture was continued with or without 10 μM fAβ_{42} for another 24 hrs. The supernatants were obtained and their contents of NO were measured by the Griess reaction as described in the Materials and Methods. The ratios of NO production of each group to the control group (untreated condition) were shown. Mean ± S.D. values were obtained from a single experiment in triplicate. Similar results were obtained in two separate experiments. *$p < 0.01$ analyzed by least significant difference test in ANOVA. NS, not significant.

Discussion

Microglia represent the brain innate immune system and hence the first line of defense against

invading pathogens and serve as specialized sensors for brain tissue injury (Streit et al. 2005; Conde and Streit 2006). Under pathological situations, such as neurodegenerative disease, microglia become activated, migrate to and surround damaged or dead cells, and subsequently clear cellular debris from the area, similar to the phagocytic active macrophages of the peripheral immune system (Fetler and Amigorena 2005). At the same time, activated microglia are also revealed to produce NO and some kinds of pro-inflammatory cytokines, which are considered to enhance the inflammation and exacerbate the diseases. There is considerable debate as to whether activated microglia are beneficial or harmful in AD. This may, however depend on the degree of activation. Nowadays, many researchers focused on how to inhibit microglial activation to restrain the inflammation. But it should also be noted that activated microglia are able to reduce Aβ accumulation by increasing its phagocytosis, clearance and degradation (Frautschy et al. 1998; Qiu et al. 1998; Yan et al. 2003). While an exaggerated immune response can certainly be detrimental to the CNS, increasing evidence demonstrates that a controlled inflammatory reaction in the brain can be greatly beneficial to the health and proper function of the CNS. So in the present study, we attempted to search a way through which we can make a controlled activation of microglia.

Among more than one hundred kinds of herbal medicines, JTT is well known to enhance the immunological functions (Matsumoto et al. 2000). Nowadays, since its anti-cancer effects (Dai et al. 2001; Tagami et al. 2004) and suppressive effects on toxicity of anti-cancer drugs (Sugiyama et al. 1995a, b) were confirmed, JTT is often clinically used for the treatment of cancer patients. And JTT has also been demonstrated to have influence not only on the acquired immune system but also the innate immune response related with macrophages (Chino et al. 2005). In the neurological diseases, AD has been demonstrated to be highly related with immune response and inflammation. Preliminary results from in vivo experiment in our laboratory supported that JTT administration diminished the senile plaques in AD transgenic mouse (Hara et al. unpublished observation). These findings prompted us to clarify the possible mechanism of the diminishing of senile plaques in order to search a new possible therapeutic way for AD.

First, we treated naive primary microglia with different concentrations of JTT, a dramatic morphological change from resting ramified cells to amoeboid microglia was observed, as well as decreased refraction and better adherent property, obviously in 200 and 400 μg/ml groups. This finding encouraged us to detect whether JTT activated microglia definitely.

Then the fact that JTT did activate microglia was demonstrated by the WST-1 cell proliferation assay and flow cytometric assay to check the surface expression of an activation marker CD11b. From the cell proliferation assay, JTT increased microglial proliferation and viability even though at a low concentration (10 μg/ml) with a slight concentration-dependent fashion. In the flow cytometric analysis, CD11b, a well-known activation marker of microglia/macrophages, was used. As expected, two peaks appeared obviously, similar with the LPS-treated group, indicating that the second peak represented the activated cells. These findings revealed that the Kampo formulation JTT could induce microglial proliferation and activation.

Then, important in our experiment was the phagocytosis-enhancing effect of JTT. There are very limited reports about phagocytosis-enhancing effects using crude extracts or oral administration of herbal medicine. According to the previous report (Liu et al. 2005), phagocytosis might be dissociated from inflammatory microglial activation in relation to the AD stage. So in the fAβ_{42}-phagocytosis assay, we chose a low (1 μM) fAβ_{42} concentration. Although 100 μg/ml JTT induced microglial proliferation, it showed no significant effect on fAβ_{42}-phagocytosis (p = 0.171); while 200 μg/ml JTT treatment increased the percentage of phagocytosed cells by about 80% compared to the unstimulated group, indicating that to show phagocytosis-enhancing effect, a relatively higher concentration was needed than to induce microglial proliferation. This concen-

tration of 200 μg/ml in in vitro experiments was consistent with the dosage for human use and the previous reports about the in vitro studies of JTT (Hisha et al. 1997; Kamiyama et al. 2005). Although 12 hrs treatment was enough to enhance the phagocytosis, no time-dependent fashion was detected. In recent studies, more attention was paid on the effect of bone marrow-derived microglia on restricting senile plaque formation (Malm et al. 2005; Simard et al. 2006). In this study, using M-CSF, we induced the bone marrow stem cells or myeloid progenitor cells to differentiate to macrophages, and we found that orally administrated JTT could also enhance the phagocytosis of f$A\beta_{42}$ in BMM. However, we used a dose of 100 mg/ml according to our previous protocol. As mentioned above, this is much higher than the dosage for human use. Although animals were tolerated well with the dose, we need to repeat the experiment with lower doses.

Activated microglia can produce NO and other pro-inflammatory cytokines, most of which are considered to be detrimental to neurons, and play an important role in the pathogenesis of AD. Excessive production of NO can mediate oxidative stress as well as amplify inflammation cascade reactions. Here we examined the NO production as a representative index. In this assay, a relatively higher (10 μM) f$A\beta_{42}$ concentration was used. First, JTT treatment did not increase the NO production, but LPS and f$A\beta_{42}$ did. Second, in the presence of f$A\beta_{42}$, although JTT pre-treatment did not reduce the NO production, at least it did not increase NO. This finding and the above results indicated that with proper concentrations and time periods of treatment, JTT might induce activation and mediate phagocytosis without eliciting excessive production of neurotoxic NO in microglia/macrophages.

In summary, the results of this study demonstrated that Kampo formulation JTT could induce microglial proliferation and activation, and also enhance f$A\beta_{42}$-phagocytosis in microglia and BMM without excessive NO production. To our knowledge, this is the first report indicating that JTT has enhancing effect of f$A\beta_{42}$-phagocytosis on microglia/macrophages. These findings support our previous finding that JTT administration diminished the senile plaque in AD transgenic mouse, which might be due to the enhanced phagocytosis of Aβ by microglia, and the phagocytosis-enhancing effect of JTT might not be accompanied by excessive inflammatoty mediators' production. This is also consistent with the previous reports showing the anti-inflammatory and anti-oxidative activities of the components of JTT (Lee et al. 2003; Matsui et al. 2004). These findings suggest that JTT administration would be a potential therapeutic or preventive approach for AD. Further intensive study should be performed in order to evaluate its therapeutic effect by in vivo study and to elucidate the underline mechanism in detail.

Acknowledgments

This study was partially supported by Grant-in-Aid for Scientific Research on Priority Areas (17025056) from the Ministry of Education, Culture, Sports, Science and Technology. Huayan Liu is a fellow supported by Sasakawa Foundation. We thank Sasakawa Memorial Health Foundation and Japan China Medical Association for their kind support. We also thank Dr. A. Suzumura, M. Sawada, K. Takahashi, H. Wakita, A. Watanabe, S. Kataoka, K. Adachi, K. Yoshizaki, and K. Takeda for their kind help and discussion in this work.

References

Bae, E.A., Kim, E.J., Park, J.S., Kim, H.S., Ryu, J.H. & Kim, D.H. (2006) Ginsenosides Rg3 and Rh2 inhibit the activation of AP-1 and protein kinase A pathway in lipopolysaccharide/ interferon-γ-stimulated BV-2 microglial cells. *Planta. Med.*, **72**, 627-633.

Baltina, L.A. (2003) Chemical modification of glycyrrhizic acid as a route to new bioactive compounds for medicine. *Curr. Med. Chem.*, **10**, 155-171.

Chino, A., Sakurai, H., Choo, M.K., Koizumi, K., Shimada, Y., Terasawa, K. & Saiki, I. (2005) Juzentaihoto, a Kampo medicine, enhances IL-12 production by modulating Toll-like receptor 4 signaling pathways in murine peritoneal exudate macrophages. *Int. Immunopharmacol.*, **5**, 871-882.

Conde, J.R. & Streit, W.J. (2006) Microglia in the aging brain. *J. Neuropathol. Exp. Neurol.*, **65**, 199-203.

Cuadros, M.A. & Navascues, J. (1998) The origin and differentiation of microglial cells during development. *Prog. Neurobiol.*, **56**, 173-189.

Dai, Y., Kato, M., Takeda, K., Kawamoto, Y., Akhand, A.A., Hossain, K., Suzuki, H. & Nakashima, I. (2001) T-cell-immunity-based inhibitory effects of orally administered herbal medicine juzen-taiho-to on the growth of primarily developed melanocytic tumors in RET-transgenic mice. *J. Invest. Dermatol.*, **117**, 694-701.

Dhuley, J.N. (1999) Anti-oxidant effects of cinnamon (Cinnamomum verum) bark and greater cardamom (Amomum subulatum) seeds in rats fed high fat diet. *Indian. J. Exp. Biol.*, **37**, 238-242.

Fetler, L. & Amigorena, S. (2005) Neuroscience. Brain under surveillance: the microglia patrol. *Science*, **309**, 392-393.

Frautschy, S.A., Yang, F., Irrizarry, M., Hyman, B., Saido, T.C., Hsiao, K. & Cole, G.M. (1998) Microglial response to amyloid plaques in APPsw transgenic mice. *Am. J. Pathol.*, **152**, 307-317.

Hisha, H., Yamada, H., Sakurai, M.H., Kiyohara, H., Li, Y., Yu, C., Takemoto, N., Kawamura, H., Yamaura, K., Shinohara, S., Komatsu, Y., Aburada, M. & Ikehara, S. (1997) Isolation and identification of hematopoietic stem cell-stimulating substances from Kampo (Japanese herbal) medicine, Juzen-taiho-to. *Blood*, **90**, 1022-1030.

Ito, S., Sawada, M., Haneda, M., Fujii, S., Oh-Hashi, K., Kiuchi, K., Takahashi, M. & Isobe, K. (2005) Amyloid-β peptides induce cell proliferation and macrophage colony-stimulating factor expression via the PI3-kinase/Akt pathway in cultured Ra2 microglial cells. *FEBS. Lett.*, **579**, 1995-2000.

Ito, S., Sawada, M., Haneda, M., Ishida, Y. & Isobe, K. (2006) Amyloid-beta peptides induce several chemokine mRNA expressions in the primary microglia and Ra2 cell line via the PI3K/Akt and/or ERK pathway. *Neurosci. Res.*, **56**, 294-299.

Kamiyama, H., Takano, S., Ishikawa, E., Tsuboi, K. & Matsumura, A. (2005) Anti-angiogenic and immunomodulatory effect of the herbal medicine "Juzen-taiho-to" on malignant glioma. *Biol. Pharm. Bull.*, **28**, 2111-2116.

Keum, Y.S., Han, S.S., Chun, K.S., Park, K.K., Park, J.H., Lee, S.K. & Surh, Y.J. (2003) Inhibitory effects of the ginsenoside Rg3 on phorbol ester-induced cyclooxygenase-2 expression, NF-κB activation and tumor promotion. *Mutat. Res.*, **523-524**, 75-85.

Kopec, K.K. & Carroll, R.T. (1998) Alzheimer's β-amyloid peptide 1-42 induces a phagocytic response in murine microglia. *J. Neurochem.*, **71**, 2123-2131.

Kreutzberg, G.W. (1996) Microglia: a sensor for pathological events in the CNS. *Trends. Neurosci.*, **19**, 312-318.

Laquintana, V., Denora, N., Lopedota, A., Suzuki, H., Sawada, M., Serra, M., Biggio, G., Latrofa, A., Trapani, G. & Liso, G. (2007) *N*-Benzyl-2-(6,8-dichloro-2-(4-chlorophenyl) imidazo [1,2-*a*] pyridin-3-yl)-*N*-(6-(7-nitrobenzo [c] [1,2,5] oxadiazol-4-ylamino) hexyl) acetamide as a new fluorescent probe for peripheral benzodiazepine receptor and microglial cell visualization. *Bioconjug. Chem.*, **18**, 1397-1407.

Lee, S.J., Lee, I.S. & Mar, W. (2003) Inhibition of inducible nitric oxide synthase and cyclooxygenase-2 activity by 1,2,3,4,6-penta-O-galloyl-beta-D-glucose in murine macrophage cells. *Arch. Pharm. Res.*, **26**, 832-839.

Liu, Y., Walter, S., Stagi, M., Cherny, D., Letiembre, M., Schulz-Schaeffer, W., Heine, H., Penke, B., Neumann, H. & Fassbender, K. (2005) LPS receptor (CD14): a receptor for phagocytosis of Alzheimer's amyloid peptide. *Brain*, **128**, 1778-1789.

Malm, T.M., Koistinaho, M., Parepalo, M., Vatanen, T., Ooka, A., Karlsson, S. & Koistinaho, J. (2005) Bone-marrow-derived cells contribute to the recruitment of microglial cells in response to β-amyloid deposition in APP/PS1 double transgenic Alzheimer mice. *Neurobiol. Dis.*, **18**, 134-142.

Matsui, S., Matsumoto, H., Sonoda, Y., Ando, K., Aizu-Yokota, E., Sato, T. & Kasahara, T. (2004) Glycyrrhizin and related compounds down-regulate production of inflammatory chemokines IL-8 and eotaxin 1 in a human lung fibroblast cell line. *Int. Immunopharmacol.*, **4**, 1633-1644.

Matsumoto, T., Sakurai, M.H., Kiyohara, H. & Yamada, H. (2000) Orally administered decoction of Kampo (Japanese herbal) medicine, "Juzen-Taiho-To" modulates cytokine secretion and induces NKT cells in mouse liver. *Immunopharmacology*, **46**, 149-161.

Park, E.K., Choo, M.K., Han, M.J. & Kim, D.H. (2004) Ginsenoside Rh1 possesses antiallergic and anti-inflammatory activities. *Int. Arch. Allergy. Immunol.*, **133**, 113-120.

Qiu, W.Q., Walsh, D.M., Ye, Z., Vekrellis, K., Zhang, J., Podlisny, M.B., Rosner, M.R., Safavi, A., Hersh, L.B. & Selkoe, D.J. (1998) Insulin-degrading enzyme regulates extracellular levels of amyloid beta-protein by degradation. *J. Biol. Chem.*, **273**, 32730-32738.

Raine, C.S. (1994) Multiple sclerosis: immune system molecule expression in the central nervous system. *J. Neuropathol. Exp. Neurol.*, **53**, 328-337.

Roepstorff, K., Rasmussen, I., Sawada, M., Cudre-Maroux, C., Salmon, P., Bokoch, G., van Deurs, B. & Vilhardt, F. (2007) Stimulus dependent regulation of the phagocyte NADPH oxidase by a VAV1, rac1, and PAK1 signaling axis. *J. Biol. Chem.*, Epub ahead of print.

Rogers, J., Luber-Narod, J., Styren, S.D. & Civin, W.H. (1988) Expression of immune system-associated antigens by cells of the human central nervous system: relationship to the pathology of Alzheimer's disease. *Neurobiol. Aging*, **9**, 339-349.

Sawada, M., Imai, F., Suzuki, H., Hayakawa, M., Kanno, T. & Nagatsu, T. (1998) Brain-specific gene expression by immortalized microglial cell-mediated gene transfer in the mammalian brain. *FEBS. Lett.*, **433**, 37-40.

Shon, Y.H. & Nam, K.S. (2003) Protective effect of Astragali radix extract on interleukin 1β-induced inflammation in human amnion. *Phytother. Res.*, **17**, 1016-1020.

Simard, A.R., Soulet, D., Gowing, G., Julien, J.P. & Rivest, S. (2006) Bone marrow-derived microglia play a critical role in restricting senile plaque formation in Alzheimer's disease. *Neuron.*, **49**, 489-502.

Streit, W.J., Conde, J.R., Fendrick, S.E., Flanary, B.E. & Mariani, C.L. (2005) Role of microglia in the central nervous system's immune response. *Neurol. Res.*, **27**, 685-691.

Sugiyama, K., Ueda, H. & Ichio, Y. (1995a) Protective effect of juzen-taiho-to against carboplatin-induced toxic side effects in mice. *Biol. Pharm. Bull.*, **18**, 544-548.

Sugiyama, K., Ueda, H., Ichio, Y. & Yokota, M. (1995b) Improvement of cisplatin toxicity and lethality by juzen-taiho-to in mice. *Biol. Pharm. Bull.*, **18**, 53-58.

Suzumura, A., Mezitis, S.G., Gonatas, N.K. & Silberberg, D.H. (1987) MHC antigen expression on bulk isolated macrophage-microglia from newborn mouse brain: induction of Ia antigen expression by gamma-interferon. *J. Neuroimmunol.*, **15**, 263-278.

Tagami, K., Niwa, K., Lian, Z., Gao, J., Mori, H. & Tamaya, T. (2004) Preventive effect of Juzen-taiho-to on endometrial carcinogenesis in mice is based on Shimotsu-to constituent. *Biol. Pharm. Bull.*, **27**, 156-161.

Takahashi, K., Prinz, M., Stagi, M., Chechneva, Olga. & Neumann, H. (2007) TREM2- transduced myeloid precursors mediate nervous tissue debris clearance and facilitate recovery in an animal model of multiple sclerosis. *PLoS. Med.*, **4**, e124.

Wang, P., Zhang, Z., Ma, X., Huang, Y., Liu, X., Tu, P. & Tong, T. (2003) HDTIC-1 and HDTIC-2, two compounds extracted from Astragali Radix, delay replicative senescence of human diploid fibroblasts. *Mech. Ageing Dev.*, **124**, 1025-1034.

Weldon, D.T., Rogers, S.D., Ghilardi, J.R., Finke, M.P., Cleary, J.P., O'Hare, E., Esler, W.P., Maggio, J.E. & Mantyh, P.W. (1998) Fibrillar β-amyloid induces microglial phagocytosis, expression of inducible nitric oxide synthase, and loss of a select population of neurons in the rat CNS in vivo. *J. Neurosci.*, **18**, 2161-2173.

Yan, Q., Zhang, J., Liu, H., Babu-Khan, S., Vassar, R., Biere, A.L., Citron, M. & Landreth, G. (2003) Anti-inflammatory drug therapy alters beta-amyloid processing and deposition in an animal model of Alzheimer's disease. *J. Neurosci.*, **23**, 7504-7509.

Transduction Properties of Adenovirus Serotype 35 Vectors After Intravenous Administration Into Nonhuman Primates

Fuminori Sakurai[1], Shin-ichiro Nakamura[2,3], Kimiyo Akitomo[1], Hiroaki Shibata[2], Keiji Terao[2], Kenji Kawabata[1], Takao Hayakawa[4] and Hiroyuki Mizuguchi[1,5]

[1]Laboratory of Gene Transfer and Regulation, National Institute of Biomedical Innovation, Ibaraki City, Osaka, Japan; [2]Tsukuba Primates Research Center, National Institute of Biomedical Innovation, Tsukuba City, Ibaraki, Japan; [3]The Corporation for Production and Research of Laboratory Primates, Tsukuba City, Ibaraki, Japan; [4]Pharmaceuticals and Medical Devices Agency, Chiyoda-Ku, Tokyo, Japan; [5]Graduate School of Pharmaceutical Sciences, Osaka University, Suita City, Osaka, Japan

Adenovirus serotype 35 (Ad35) vectors have shown promise as effective gene delivery vehicles. However, the transduction profiles of Ad35 vectors in conventional mice allow only a limited estimation of transduction properties of these vectors, because the mouse analog of the subgroup B Ad receptor, CD46, is restricted to the testis. In order to assess the transduction properties of Ad35 vectors more completely, we performed transduction experiments using cynomolgus monkeys, which ubiquitously express CD46 in a pattern similar to that in humans. *In vitro* transduction experiments demonstrated that cultured cells from the cynomolgus monkey were efficiently transduced with Ad35 vectors. In contrast, after intravenous administration into live monkeys hardly any evidence of Ad35 vector–mediated transduction was found in any of the organs, although Ad35 vector genomes were detected in various organs. Less severe histopathological abnormalities were found in the Ad35 vector–infused monkeys than in the conventional Ad5 vector–injected monkeys. In the latter, serious tissue damage and inflammatory responses, such as hepatocyte necrosis and lymphatic hyperplasia in the colon, were induced. Both Ad35 and Ad5 vectors caused similar hematological changes (increase in $CD3^+$ cells, and decrease in $CD16^+$ cells and $CD20^+$ cells) in peripheral blood cells. These results should provide valuable information for the clinical application of Ad35 vectors.

Received 15 September 2007; accepted 16 January 2007; advance online publication 11 March 2008. doi:10.1038/mt.2008.19

INTRODUCTION

Human adenoviruses (Ads) are nonenveloped, double-stranded DNA viruses that are composed of 51 serotypes.[1,2] Among the 51 serotypes, the conventional Ad vectors that are most widely used, including for human clinical trials, are constructed based on the subgroup C Ad serotype 5 (Ad5). Ad5 vectors have several advantages as gene delivery vehicles, but clinical and preclinical studies have revealed three major disadvantages of Ad5 vectors. First, target cells that are important for gene therapy, including malignant tumor cells and dendritic cells, express nil or insufficient levels of a cellular receptor for Ad5, the coxsackievirus-adenovirus receptor. The transduction efficiencies of Ad5 vectors depend to a large extent on the expression levels of coxsackievirus-adenovirus receptor, leading to refractoriness of coxsackievirus-adenovirus receptor-negative cells to Ad5 vectors.[3] Second, >50% of adults are seropositive for Ad5 because natural infection with Ad5 is common.[4,5] Pre-existing anti-Ad5 antibodies not only largely inhibit Ad5 vector–mediated transduction, but may also enhance the toxicities induced by Ad5 vectors.[6] Third, inflammatory responses are systemically and rapidly induced by intravascular administration of Ad5 vectors, leading to tissue damage, and this can be fatal to the host.[7–10]

In order to address these problems, we as well as others have developed a replication-incompetent subgroup B Ad serotype 35 (Ad35) vector.[11–15] Ad35 vectors utilize human CD46 as a cellular receptor.[16,17] Human CD46 is ubiquitously expressed on almost all human cells, leading to a wide tropism of Ad35 vectors. In addition, pre-existing anti-Ad5 immunity does not hamper Ad35 vector–mediated transduction, and seroprevalence for Ad35 is much lower than that for Ad5 (refs. 13,14). Ad35 vectors have properties that make them very promising prospects for use as transduction vehicles, but the transduction efficiencies of Ad35 vectors in conventional mice are lower than those of Ad5 vectors.[12,14] Conventional mice seem inappropriate as animal models for Ad35 vectors because mouse CD46 is expressed only in the testis.[18] In addition, there is low homology between human CD46 and mouse CD46. We considered that transduction experiments with Ad35 vectors should be performed using nonhuman primates so as to properly evaluate the transduction properties of Ad35 vectors. The CD46 of nonhuman primates is ubiquitously expressed in a similar pattern to humans, and shows high homology to human CD46.[19]

In this study, we examined the transduction profiles of Ad35 vectors after intravenous administration into nonhuman primates, *i.e.*, cynomolgus monkeys. Ad35 vector–induced immune responses and the blood concentrations of Ad35 vectors were

Correspondence: Hiroyuki Mizuguchi, Laboratory of Gene Transfer and Regulation, National Institute of Biomedical Innovation, 7-6-8 Asagi, Saito, Ibaraki City, Osaka 567-0085, Japan. E-mail: mizuguch@nibio.go.jp

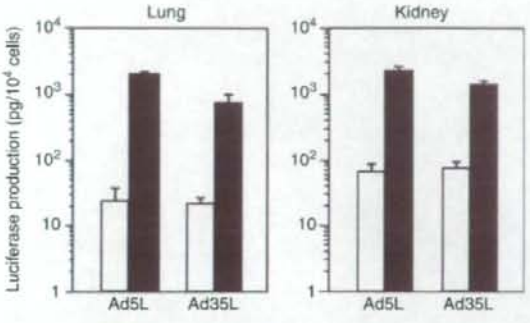

Figure 1 *In vitro* transduction efficiencies of Ad35 and Ad5 vectors in cultured cells of cynomolgus monkey. Luciferase production in primary lung and kidney cells following Ad vector transduction. Primary lung and kidney cells isolated from cynomolgus macaque embryos were transduced with Ad35L or Ad5L at 300 (open bar) and 3,000 vector particles/cell (closed bar) for 1.5 hours. After a 48-hour culture, luciferase production in the cells was measured by luminescence assay. The data are expressed as the mean values ± SD ($n = 4$). Luciferase expression in the mock-infected cells was less than the detectable level. Ad, adenovirus.

analyzed for 4 days after the injection. Necropsy was performed 4 days after the injection to examine the transduction efficiencies, tissue accumulations of Ad35 vectors, and histopathological changes in the organs after injection.

RESULTS

In vitro transduction in cultured cynomolgus monkey cells

First, to examine whether cynomolgus monkey cells were susceptible to Ad35 vectors, primary lung and kidney cells isolated from embryonic cynomolgus monkeys were transduced with a firefly luciferase-expressing Ad35 vector (Ad35L) and a conventional Ad5 vector (Ad5L). Both Ad35L and Ad5L vectors were shown to mediate efficient transduction in the cells from both organs (**Figure 1**). Ad35 vectors also efficiently transduced the cynomolgus monkey T-cell line HSC-F (**Supplementary Figure S1**). These results indicate that cynomolgus monkey cells are susceptible to Ad35 vectors. However, peripheral blood mononuclear cells of cynomolgus monkeys were almost refractory to Ad35 vectors (data not shown).

Blood clearance of Ad vectors

Next, the six cynomolgus monkeys (designated #1–#6) were administered either a β-galactosidase-expressing Ad35 vector (Ad35LacZ) or an Ad5 vector (Ad5LacZ) through the femoral vein (**Supplementary Table S1**). The blood clearances of the Ad vectors were examined using a quantitative real-time polymerase chain reaction. Both Ad35LacZ and Ad5LacZ vectors were rapidly cleared from the blood circulation within 24 hours after the injection (**Figure 2a** and **b**). We did not find any apparent differences between the blood-clearance kinetics of Ad35LacZ and Ad5LacZ. Assuming that the entire Ad vector DNA in the blood was completely recovered from the blood samples, there would remain 0.12% and 0.09% of the injected Ad35LacZ in the blood of monkey #6 at 3 and 6 hours after injection, respectively. The lower levels of

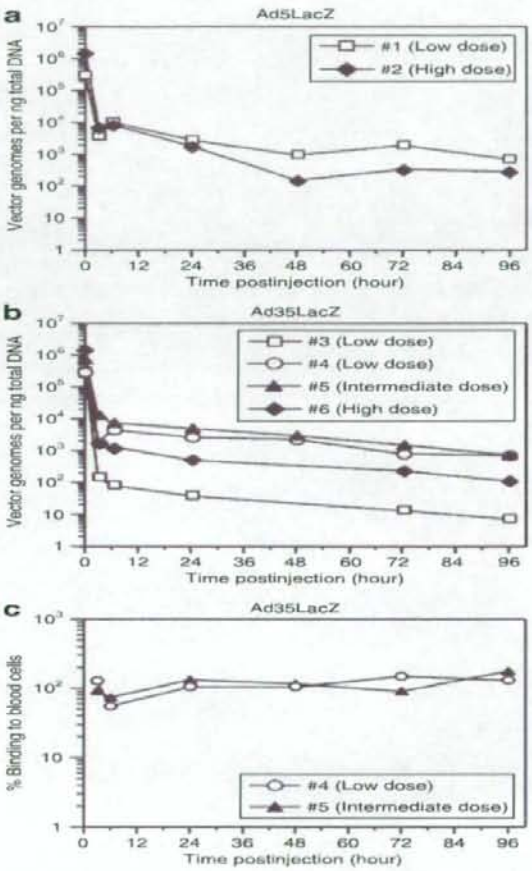

Figure 2 Persistence of adenoviral (Ad) vectors in the blood of cynomolgus monkeys following systemic administration. (**a**) Ad vector DNA concentrations in the blood after intravenous administration. Cynomolgus monkeys were intravenously infused with Ad35LacZ or Ad5LacZ at low [0.4×10^{13} vector particles (VP)/kg], intermediate (1.0×10^{13} VP/kg), or high (2×10^{13} VP/kg) doses. Blood was collected at the indicated time points after injection (3, 6, 24, 48, 72, and 96 hours after injection). Total DNA, including Ad vector DNA, was isolated from the blood, and the Ad vector DNA contents were measured using quantitative TaqMan polymerase chain reaction (PCR) assay. The concentrations of the Ad vectors in the blood at the zero time point were calculated based on the total number of Ad vector particles infused and the estimated circulating blood volume (65 ml/kg). Ad vector DNA was not detected in the blood before injection. (**b**) Percentages of blood cell–associated Ad35lacZ remaining in the blood after systemic administration in cynomolgus monkeys. After isolating the blood as described, blood cells were washed twice with phosphate-buffered saline buffer and the amounts of Ad35LacZ associated with blood cells were evaluated using TaqMan PCR as described earlier. The percentages were calculated as follows: 100 × (the amounts of Ad35 vector DNA associated with blood cells)/(the amounts of Ad35 vector DNA recovered from whole blood).

Ad35LacZ remaining in the blood of monkeys #3 and #6 than those in monkeys #4 and #5 might have been partly because of the low infectious titer-to-particle ratio of the vector batch of Ad35LacZ injected into monkeys #3 and #6. The infectious titer-to-particle

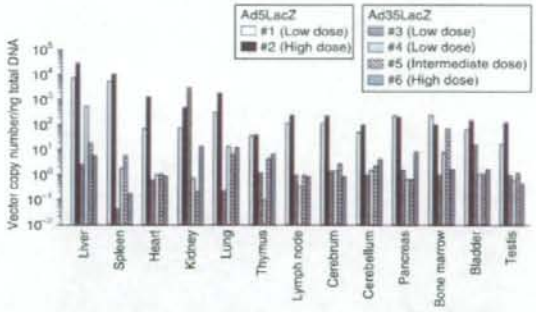

Figure 3 *In vivo* tissue distributions of adenoviral (Ad) vector DNA in cynomolgus monkeys after systemic administration. Ad35LacZ or Ad5LacZ was intravenously administered into cynomolgus monkeys as described for **Figure 2**. Four days after the injection, necropsy was performed, and Ad vector DNA contents were measured using quantitative TaqMan polymerase chain reaction analysis. The Ad vector DNA was not detected in the organs of mock-infected animals.

ratio of the Ad35LacZ used in monkeys #3 and #6 was lower than that used in monkeys #4 and #5 (data not shown). Noninfectious Ad particles might be more easily degraded in the blood or taken up by phagocytic cells.

Further, we examined whether the Ad35 vectors were associated with blood cells in the blood stream after the injection. The majority of Ad35LacZ remaining in the blood was associated with blood cells at all the time points (**Figure 2c**). Similarly, assuming the complete recovery of the Ad vector DNA as described earlier, 1.5% of the injected Ad35LacZ would be associated with blood cells in monkey #5 at 3 hours after the injection. The levels of Ad35LacZ associated with blood cells remained constant during the study. These results suggest that Ad35 vectors may bind to blood cells, or be taken up by blood cells after the injection.

Tissue distribution of Ad vectors

In order to examine the biodistribution of Ad35 and Ad5 vectors in cynomolgus monkeys after intravenous administration, Ad DNA contents in the organs were assessed (**Figure 3**). The Ad35 vector DNA was mainly found in the liver, lung, and kidney; however, the levels of Ad35 vector DNA were one to five orders of magnitude lower in almost all organs than the levels of Ad5 vector DNA, which was found mainly in the liver and spleen. Ad35LacZ was also less efficiently accumulated in the organs that exhibited low levels of Ad5LacZ accumulation, such as the thymus and testis.

Ad vector–mediated transgene expression in organs

In order to evaluate the *in vivo* transduction efficiencies of Ad35 and Ad5 vectors, β-galactosidase expression in the organs was examined. Ad5LacZ efficiently transduced the organs (**Figure 4a**). The highest level of β-galactosidase production was found in the liver, followed by the spleen. Liver parenchymal cells and spleen marginal zone cells were mainly transduced by Ad5LacZ in these organs (**Figure 4b**). On the other hand, Ad35 vector–mediated β-galactosidase expression in the organs at all doses was approximately equal to, or slightly above, the levels in

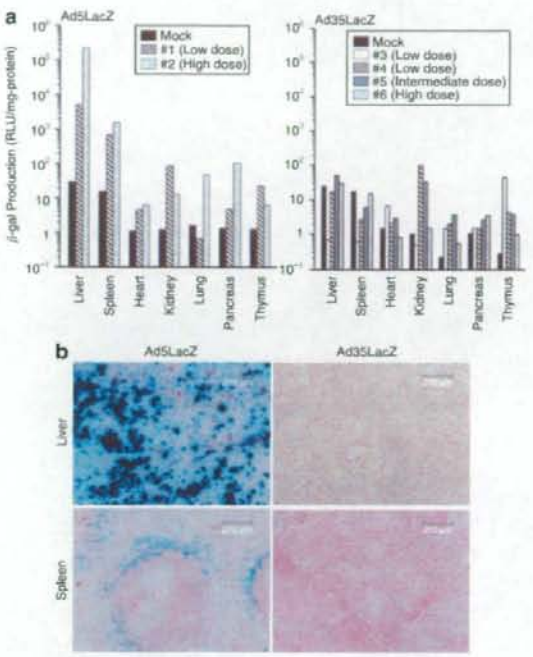

Figure 4 Adenoviral (Ad) vector–mediated transgene expression in cynomolgus monkeys after systemic administration. (**a**) Chemiluminescence analysis of β-galactosidase production in cynomolgus monkeys after systemic administration of Ad35LacZ or Ad5LacZ. Ad35LacZ or Ad5LacZ was intravenously injected into cynomolgus monkeys as described for **Figure 2**. Four days after injection, the organs were collected, and β-galactosidase production in the organs was assessed using a chemiluminescence assay. (**b**) X-gal staining of tissue sections of cynomolgus monkeys receiving Ad5LacZ or Ad35LacZ. Four days after intravenous administration of Ad35LacZ or Ad5LacZ at a high dose (2×10^{12} vector particles/kg), tissues were collected, and X-gal staining was performed as described in Materials and Methods. RLU, relative light units.

mock-infected animals. X-gal-positive cells were not found in the tissue sections of the liver or spleen of the Ad35LacZ-infused monkeys. These results indicate that Ad35 vectors show much lower transduction activity than Ad5 vectors after systemic delivery in cynomolgus monkeys.

Serum chemistry profiles

Next, we measured the levels of serum biochemical markers to assess Ad vector–induced tissue/organ damage. Almost all the markers were increased following Ad vector injection; however, overall, the markers examined appeared to be more elevated in the monkeys receiving Ad5LacZ than in those receiving Ad35LacZ (**Figure 5a**). Aspartate aminotransferase (AST) levels were elevated as early as 3 hours after the injection, and peaked at 24 hours in most cases. The peak levels of AST in Ad35LacZ-injected monkeys #3, #4, #5, and #6 were 6.1-, 4.8-, 8.2-, and 3.8-fold higher than the preinjection levels, respectively. By contrast, Ad5LacZ-infused monkeys (#1 and #2) showed 4.9- and 27.5-fold increases in AST at the peak points, respectively. Significant elevations in alanine

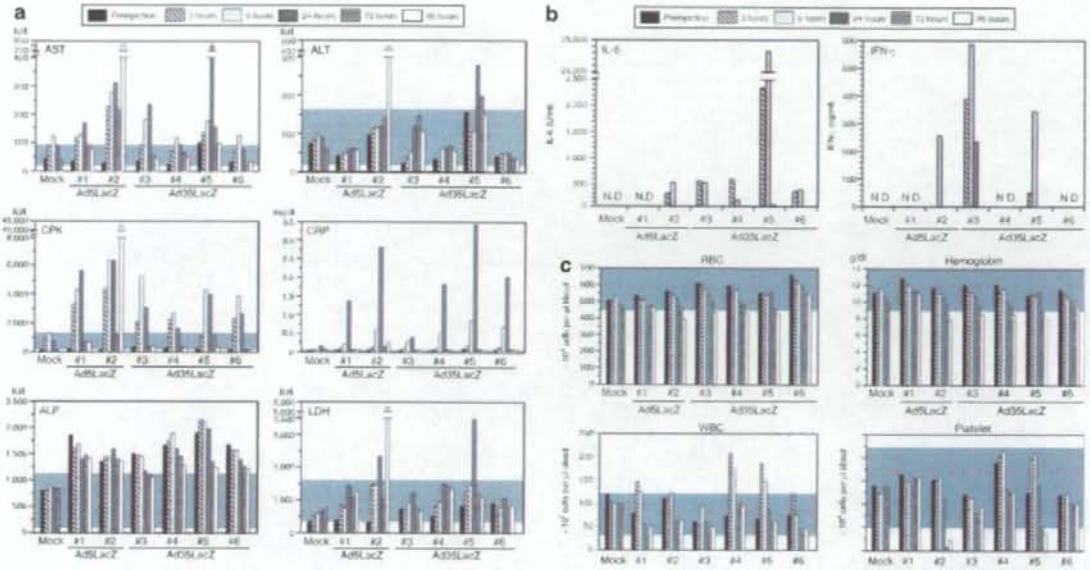

Figure 5 Blood analysis after adenoviral (Ad) vector administration to cynomolgus monkeys. (**a**) Serum marker levels, (**b**) inflammatory cytokine productions, and (**c**) blood cell counts in the peripheral blood after Ad vector administration. The gray area in the graphs of serum markers and blood cell counts indicates the normal range for adult cynomolgus monkeys. Ad35LacZ or Ad5LacZ was intravenously injected into cynomolgus monkeys and blood was collected as described for **Figure 2**. Serum marker levels and blood cell counts were measured using routine methods. Inflammatory cytokine levels were examined using enzyme-linked immunosorbent assay. ALT, alanine aminotransferase; AST, aspartate aminotransferase; CPK, creatine phosphokinase; CRP, C-reactive protein; IFN-γ, interferon-γ; IL-6, interleukin-6; LDH, lactate dehydrogenase; ND, not detected (under the limit of detection); RBC, red blood cell; WBC, white blood cell.

aminotransferase were also found in several of the monkeys, but the alanine aminotransferase levels were within the normal range at almost all the time points. Creatine phosphokinase (CPK) levels sharply rose to a peak 6 or 24 hours after injection. CPK in the Ad35 vector–injected monkeys #3, #4, #5, and #6 showed 14.2-, 9.7-, 16.3-, and 17.7-fold increases at the peak points. On the other hand, the Ad5 vector–injected monkeys #1 and #2 exhibited 16.6- and 40.9-fold elevations in CPK at 6 hours after the injection. Dramatic increases in AST, alanine aminotransferase, and CPK levels in monkey #2 at 96 hours after injection was possibly caused by a slight expression of Ad5 E2 and/or E4 proteins. E4 protein was expressed in the liver 4 days after injection of conventional Ad vectors in mice, leading to liver damage.[20] Levels of C-reactive protein were also sharply increased in all the Ad vector–injected animals. A high dose of Ad35LacZ and Ad5LacZ caused 29-fold (#6) and 56.2-fold (#2) increases in C-reactive protein levels 24 hours after injection, respectively. Alkaline phosphatase levels gradually decreased over the first 96 hours after injection. Alkaline phosphatase levels at preinjection were higher than the normal range in the monkeys. This is because young cynomolgus monkeys (<4 years of age) often have alkaline phosphatase levels >1,000 IU/L. Apparent increases in lactate dehydrogenase were found in monkeys #2 and #5. The lactate dehydrogenase levels in the other animals were within the normal range. There were no abnormalities in the other parameters, including serum albumin, glucose, cholesterol, calcium, sodium, potassium, and chloride (data not shown).

Inflammatory cytokine induction

In order to examine the innate immune responses after Ad vector injection, inflammatory cytokine levels in the serum were measured (**Figure 5b**). Interleukin-6 (IL-6) was rapidly induced with a peak at 3 or 6 hours after the injection in all the animals except in monkey #1. There were no apparent differences in IL-6 levels between Ad35LacZ-treated and Ad5LacZ-treated animals, except that monkey #5 produced an extremely high level of IL-6. The levels of interferon-γ were also elevated and reached a peak at 6 hours after the injection in monkeys #2, #3, and #5. Tumor necrosis factor-α was not detected in any of the animals (data not shown).

Hematological profiles

In order to evaluate the influence of Ad vector injection on the hematological profiles, we examined the changes in peripheral blood cell counts (**Figure 5c**). The changes in the levels of red blood cells and hemoglobin were marginal, but the levels gradually decreased after injection in all the monkeys, including a mock-infected animal, probably because of the collection of large volumes of blood samples (>5 ml/time point) every day. Ad35LacZ-injected monkeys #3, #4, and #5, and Ad5LacZ-injected monkey #2 showed a rapid decline in platelet levels beginning at 24 hours after the injection. A transient increase in the platelet levels was found 3 and 6 hours after the injection in monkey #5. It remains unclear why the platelet levels increased in monkey #5; however, the previous study also reported an initial increase in the platelet levels after Ad5 vector injection in nonhuman primates.[21] A rapid

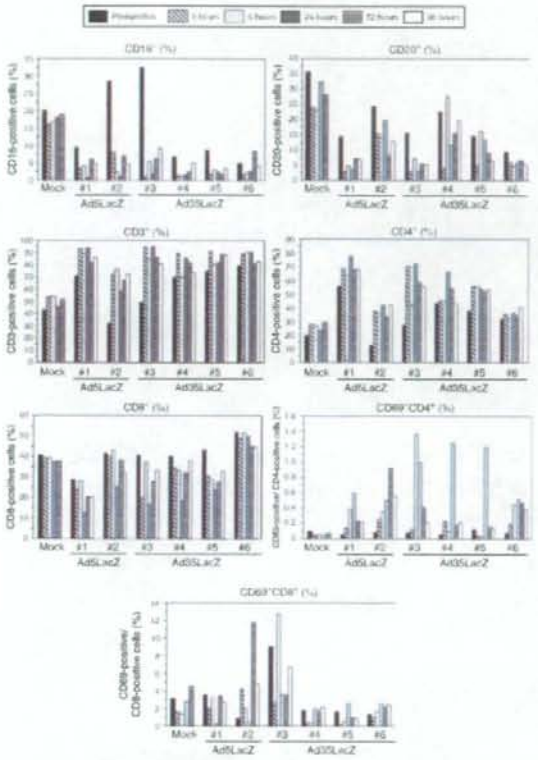

Figure 6 Profiles of peripheral blood lymphocyte subsets after systemic administration of adenoviral (Ad) vectors in cynomolgus monkeys. Ad35LacZ or Ad5LacZ was intravenously injected into cynomolgus monkeys and blood was collected as described for **Figure 2**. Peripheral blood mononuclear cells were stained with monoclonal antibodies following hemolysis, and fluorescence-activated cell sorting analysis was performed for evaluation of profiles of lymphocyte subsets.

elevation in the white blood cells was observed in the Ad vector–injected monkeys. The elevated white blood cells level returned to normal at 24 hours after the injection.

Next, we examined which types of blood cells were increased or decreased after Ad vector injection (**Figure 6**). The Ad vector injection induced a rapid decline in the percentages of $CD16^+$ cells (natural killer cells, granulocytes, and monocytes). Monkeys #2 and #3 showed sharp decreases of 71 and 97% of $CD16^+$ cells, respectively, at 3 hours after the injection. The percentages of $CD20^+$ cells (B cells) quickly dropped in all the monkeys, including a mock-infected monkey. In contrast, the $CD3^+$ cell (T-cell) levels were sharply elevated in the animals receiving the Ad vectors. We found a 1.1- to 2.3-fold increase in $CD3^+$ cell levels at 3 hours after the injection. $CD8^+$ cells did not increase, but rather decreased after the injection; however, increases in $CD4^+$ cells were found in the Ad vector–injected monkeys. The $CD4^+$ cell levels were 1.1- to 3.4-fold elevated compared with the preinjection levels, with a peak at 24 hours after the injection, in most of the animals. The administration of Ad vectors also increased

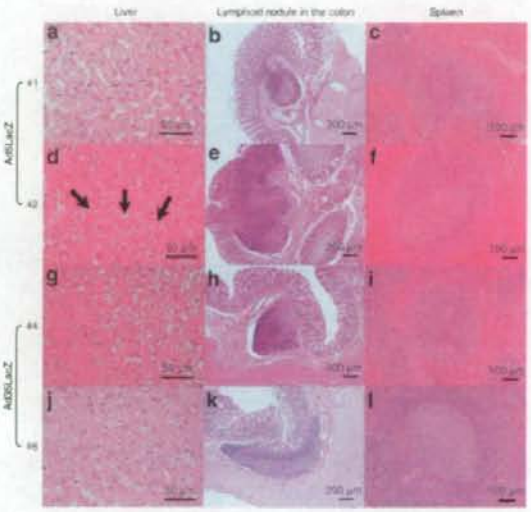

Figure 7 Histopathological analysis of liver, lymphoid nodules in the colon, and spleen. Representative histological sections of the liver (**a**, **d**, **g**, **j**), lymphoid nodules in the colon (**b**, **e**, **h**, **k**), and spleen (**c**, **f**, **i**, **l**) from animals killed 4 days after systemic injection of a low or high dose of Ad35LacZ (monkeys #4 and #6) or Ad5LacZ (#1 and #2). The arrows indicate necrosis of hepatocytes.

$CD69^+CD4^+$ cells (activated $CD4^+$ cells) more predominantly than $CD69^+CD8^+$ cells. Both $CD29^+CD4^+$ cells (memory helper T cells) and $CD29^-CD4^+$ cells (naive helper T cells) increased in the Ad vector–injected animals (data not shown). These results indicate that, overall, both Ad35 and Ad5 vectors cause similar changes in hematological profiles after systemic infusion.

Clinical observation and histopathological examinations

In order to perform a safety assessment of the Ad vectors, the health condition of the animals was monitored until necropsy. None of the Ad vector–infused monkeys showed any apparent abnormalities in appetite, body weight, body temperature, or heart rate. However, the low dose of Ad35LacZ (#3) induced vomiting 3 hours after the injection, and a skin rash was observed in monkey #2 on day 2.

In order to further evaluate the safety profiles of Ad vectors, organ histopathology was examined during necropsy. There were no obvious changes in the spleens of monkeys #1 and #3–#6, or in the livers in any of the animals. However, splenomegaly was found in monkey #2. The whitish nodules at the cut surface of the spleen in monkey #2 were the largest among those of all the monkeys examined. Marked swelling of the lymph nodules, especially in the colon and mesentery, was also found in monkey #2.

Microscopic analysis of tissue sections revealed that no apparent damage and inflammation were found in the liver of monkey #1 (**Figure 7a**). Although slight hyperplasia in the spleen white pulp occurred in this monkey (**Figure 7c**), no obvious changes were found in the lymphatic nodules of the colon (**Figure 7b**). In contrast, severe damage and inflammation, including necrosis of hepatocytes (**Figure 7d**, arrows) and infiltration of lymphocytes

into the Glisson's sheath (data not shown) were found in monkey #2. Furthermore, apparent severe hyperplasia in the lymphoid nodules of the colon (**Figure 7e**) and spleen white pulp (**Figure 7f**) had been induced in monkey #2. On the other hand, the livers of Ad35LacZ-treated monkeys exhibited almost no damage or inflammation (**Figure 7g** and **j**). In addition, Ad35LacZ induced hyperplasia in lymphoid nodules of the colon (**Figure 7h** and **k**) was only slightly developed and less serious than that induced by the high dose of Ad5LacZ. These results suggest that Ad5 vectors may cause more severe damage and/or inflammation in the liver and lymphoid nodules of the colon than Ad35 vectors. The spleen white pulp developed only slight hyperplasia in monkey #4 (**Figure 7i**), in contrast, the high dose of Ad35LacZ induced severe hyperplasia in the spleen white pulp (**Figure 7l**). The level of hyperplasia in spleen white pulp of monkey #6 appeared to be slightly more severe than that of monkey #2. The monkeys #3 and #5 did not show apparent abnormalities in the spleen or colon, although slight vacuolation in hepatocytes and infiltration of lymphocytes in the Glisson's sheath was found (data not shown). Hyperplasia in spleen white pulp and lymphatic follicles in the mesenteric, axillary, and inguinal lymph nodes (data not shown) occurred dose-dependently in the Ad35-injected animals as well as in the Ad5-injected ones.

DISCUSSION

In this study, subgroup B Ad35 vectors were intravenously infused into cynomolgus monkeys in order to evaluate the *in vivo* fundamental transduction properties of Ad35 vectors more thoroughly. Cynomolgus monkey CD46 and the CD46 of other nonhuman primates, have significant homology with human CD46 (ref. 19). In particular, short consensus repeats 1 and 2 (which are crucial for Ad35 binding to CD46),[22–24] of the CD46 of the cynomolgus monkey show high homology (85%) with those in human CD46. In addition, we confirmed that the monkey cells used in this study were highly stained with anti-human CD46 monoclonal antibody M177, which is specific for short consensus repeat 2, and that the antibody M177 significantly inhibited Ad35 vector–mediated transduction in the cynomolgus monkey cells (data not shown). The amino acid sequences important for Ad35 binding to CD46 (refs. 23,24) are also well conserved in cynomolgus monkey CD46. These results indicate that cynomolgus monkey CD46 serves as a cellular receptor for Ad35, at least in the context of *in vitro* transduction.

In this study, four and two cynomolgus monkeys were intravenously injected with the Ad35 and Ad5 vectors, respectively. We must exercise caution in interpreting the results because the sample size is small, as is natural in nonhuman primate studies. Overall, there are no dose responses in several transduction profiles of both Ad35 and Ad5 vectors, including blood concentration of Ad vectors and inflammatory cytokine production. The variations in the transduction profiles suggest that these profiles may depend largely on the specific Ad vector batch and on the differences between individuals, such as health conditions and genetic backgrounds, as well as on Ad vector doses. In the clinical trials using Ad vectors, inflammatory responses were dramatically different between patients receiving the same vector dose.[31] Gene therapy studies, both preclinical and clinical, should be performed with considerable caution in view of these individual differences. Further studies, including toxicogeomics, would be necessary in order to clarify which parameters play the most crucial roles in this entire process of transduction. Such studies would enable prediction of profiles of Ad vector–mediated transduction, and associated toxicities.

Although efficient transduction was achieved using Ad35 vectors *in vitro*, transduction of Ad35 vectors in the organs *in vivo* was hardly detectable after systemic infusion (**Figure 4**). In addition, the levels of Ad35 vector genome in the organs were one to five orders lower than those of the Ad5 vector genome (**Figure 3**). Previous studies demonstrated that, after systemic injection, Ad35 vectors were poor at transducing CD46-transgenic (CD46TG) mice, which ubiquitously express human CD46 in all the organs.[15,26] Chimeric Ad5 vectors containing Ad35 fiber protein also mediated much lower transgene expression in baboons than conventional Ad5 vectors did.[27] These results indicate that Ad35 vectors cannot transduce organs efficiently when introduced into the blood stream. There are two possible explanations for the poor transduction activity of Ad35 vectors after systemic administration. First, Ad35 vectors might be more susceptible than Ad5 vectors to degradation in the blood or in intracellular compartments such as endosomes/lysosomes after internalization. Fiber-substituted Ad5 vectors containing a fiber protein of Ad35 remain for a longer time in late endosome/lysosomal compartments after internalization than Ad5 vectors do.[28] Ad35 vectors might exhibit similar intracellular trafficking to the fiber-substituted Ad5 vectors, leading to high susceptibility to intracellular degradation. Second, Ad35 vectors might not be able to gain access to CD46 after systemic injection. CD46 is predominantly expressed on the basolateral sides of cells,[29,30] making it inaccessible to Ad35 vectors. Ad35 vectors which are not able to bind to CD46 on the cell surface would be phagocytosed into phagocytic cells, such as liver Kupffer cells, leading to degradation.

It is well known that erythrocytes of cynomolgus monkeys express CD46 (ref. 19) and that Ad35 causes hemagglutination of monkey erythrocytes.[31] Ad35 vectors might induce hemagglutination in the blood vessels after the injection, and this might lead to hemolysis and a decrease in the transduction efficiencies of Ad35 vectors. A large percentage of the Ad35 vectors recovered from the blood after the injection were associated with blood cells (**Figure 2c**). However, lactate dehydrogenase (a marker of hemolysis) levels in the sera of Ad35LacZ-injected animals at most of the time points were within normal levels and comparable with those in the sera of animals injected with Ad5LacZ, which does not induce hemagglutination of monkey erythrocytes. These results suggest that hemagglutination by Ad35 vectors would have, at most, a minimal influence on the transduction profiles of Ad35 vectors.

As mentioned earlier, CD46TG mice as well as cynomolgus monkeys were only poorly transduced with Ad35 vectors after intravenous administration, thereby suggesting that the transduction profiles of Ad35 vectors in CD46TG mice would correspond to those in primates and that CD46TG mice might be suitable as a small animal model for the study of Ad35 vectors. The profiles of inflammatory cytokine production by Ad35 vectors in cynomolgus monkeys were also approximately similar to those in CD46TG mice. Intravenous

infusion of Ad35 vectors resulted in levels of inflammatory cytokine production comparable to those induced by Ad5 vectors in the monkeys (**Figure 5b**) as well as in CD46TG mice.[32]

Histopathological analysis demonstrated that tissue damage and inflammatory responses, including hepatocyte necrosis, were less severe in all the Ad35 vector-infused monkeys than in the Ad5 vector-injected ones (**Figure 7**). Previous studies also demonstrated that Ad35 vectors are less immunogenic than Ad5 vectors in mice,[33,34] and this may result in the higher safety profiles of Ad35 vectors as compared to Ad5 vectors. It remains to be elucidated why Ad35 vectors produce less severe side effects than Ad5 vectors. Ad5 vectors were more widely distributed in most organs than Ad35 vectors, suggesting that Ad5 vectors may cause tissue damage and inflammatory responses throughout the whole body. On the other hand, Ad35LacZ induced much higher levels of IL-6 and interferon-γ in monkeys #5 and #3, respectively, than in the other Ad35LacZ-infused monkeys (**Figure 5b**), although no severe damage or inflammation was observed in these two animals. It remains unclear why such high levels of inflammatory cytokines were induced by Ad35 vectors in these animals; however, previous studies have indicated that the high levels of inflammatory cytokine induction might be involved in tissue damage.[8,35] It is important to pay attention to Ad35 vector-induced innate immune responses.

The poor transduction efficiencies of Ad35 vectors in organs after systemic administration could constitute another potential advantage in their use, namely, that locally administered Ad35 vectors would not cause unwanted side effects in organs other than the targeted organs, when draining from injected sites into the blood stream. This is in contrast to Ad5 vectors which, after injection into local tissues, have been shown to drain into the blood stream in large quantities and cause unwanted side effects in the liver and other organs.[36,37] We previously demonstrated that intramuscular injection of Ad35 vectors led to efficient transduction at the injected sites,[12] and thus local injection of Ad35 vectors would be expected to mediate efficient transduction at the injected sites without side effects in other organs.

In summary, we have demonstrated the transduction properties of Ad35 vectors after intravenous administration in nonhuman primates. Systemic infusion of Ad35 vectors did not result in detectable levels of transgene expression in the organs. Also, the tissue damage was less severe in the animals receiving Ad35 vectors than in those receiving Ad5 vectors, although two monkeys produced marked inflammatory cytokines after receiving Ad35 vectors. Further studies are in progress, focusing on the local injection of Ad35 vectors, and the results of these studies may further clarify the potential utility of Ad35 vectors.

MATERIALS AND METHODS

Ad vectors. An Ad5 vector and an Ad35 vector containing a β-galactosidase expression cassette, Ad5LacZ and Ad35LacZ, respectively, were prepared using an improved *in vitro* ligation method.[38–40] Briefly, for preparation of Ad5LacZ, pHMCMV6-LacZ, which was constructed by insertion of the β-galactosidase gene derived from pCMVβ (Clontech, Palo Alto, CA) into pHMCMV6,[39] was digested with I-*Ceu*I and PI-*Sce*I, and then ligated with I-*Ceu*I- and PI-*Sce*I-digested Ad5 vector plasmid pAdHM4.[39] The resulting plasmid was digested with *Pac*I and transfected into 293 cells with Superfect (Qiagen, Valencia, CA). The vector plasmid for Ad35LacZ was constructed in a similar manner, but using pHMCMV6-LacZ and pAdMS18.[35] The resulting plasmid was digested with *Sbf*I and transfected into 293-E1B cells,[35] which are a 293 transformant stably expressing Ad35 E1B-55K protein. The viruses were prepared using a standard method, and purified by $CsCl_2$ step gradient ultracentrifugation followed by $CsCl_2$ linear gradient ultracentrifugation. Determination of virus particle titers was accomplished spectrophotometrically using the methods of Maizel *et al.*[41] Luciferase-expressing Ad5 and Ad35 vectors, Ad5L and Ad35L, were constructed as explained earlier.[11]

In vitro *transduction.* Lung and kidney primary cells, isolated from embryonic cynomolgus monkeys and cultured in Roswell Park Memorial Institute-1640 medium supplemented with 10% fetal bovine serum, antibiotics, and L-glutamine, were seeded in a 96-well dish at 1×10^5 cells/well. On the following day, they were transduced with Ad5L or Ad35L at 300 and 3,000 vector particles/cell for 1.5 hours. After a 48-hour culture period, luciferase production in the cells was measured using a luciferase assay system (PicaGene LT2.0; Toyo Inki, Tokyo, Japan).

Animals. Young male cynomolgus monkeys (*Macaca fascicularis*) were housed and handled in accordance with the rules for animal care and management of the Tsukuba Primate Center and the guiding principles for animal experiments using nonhuman primates formulated by the Primate Society of Japan. The animals (~3 years of age, 1.88–2.96 kg) were certified free of intestinal parasites and seronegative for simian type-D retrovirus, herpesvirus B, varicella-zoster-like virus, and measles virus. The protocol of the experimental procedures was approved by the Animal Welfare and Animal Care Committee of the National Institute of Biomedical Innovation (Osaka, Japan).

In vivo *transduction.* Cynomolgus monkeys were sedated with ketamine (5–10 mg/kg) and injected with phosphate-buffered saline (mock), or Ad5LacZ or Ad35LacZ at 2×10^{12} vector particles/kg (high dose), 1×10^{12} vector particles/kg (intermediate dose), or 0.4×10^{12} vector particles/kg (low dose) through the saphenous vein at a rate of ~2 ml/minutes. Blood was collected for analysis at 3, 6, 24, 48, 72, and 96 hours after injection. Four days after vector administration, the monkeys were killed and the tissues were collected. Tissue samples were subjected to analysis as described in the later text.

β-Galactosidase assay and X-gal staining. β-Galactosidase activity in the organs was measured using Galacto-Light Systems (Applied Biosystems, Foster City, CA) as earlier described.[37] Protein concentrations were determined with a Bio-Rad assay kit (Bio-Rad, Hercules, CA) using bovine serum albumin as a standard. X-gal staining of tissue sections was performed as earlier described.[41]

Blood clearance and tissue distribution of Ad vectors. Blood clearance analysis of Ad vectors was performed using a real-time polymerase chain reaction assay, as earlier described.[8,40] Briefly, total DNA, including the Ad vector DNA, was isolated from whole blood samples. After isolation, the total DNA concentrations were determined, and the Ad DNA contents were quantified using a TaqMan fluorogenic detection system (ABI Prism 7700 sequence detector; Perkin-Elmer Applied Biosystems, Foster City, CA).

The association of Ad35 vectors to blood cells circulating in the blood stream was evaluated using a real-time polymerase chain reaction assay. Blood samples collected at the indicated time points were washed two times with phosphate-buffered saline immediately after isolation to remove unbound Ad35 vectors. After washing, total DNA was extracted from blood cells and the Ad35 DNA contents were assessed as described earlier.

The Ad DNA contents in each organ were similarly quantified using a real-time polymerase chain reaction assay, as described earlier, after isolation of the total DNA from each organ using a Automatic Nucleic Acid Isolation System (NA-2000; KURABO, Osaka, Japan).

Histopathology. For routine histopathology, tissues were fixed in 10% formalin at the time of necropsy, and processed for paraffin embedding.

Sections of 4-μm thickness were cut and stained with hematoxylin and eosin. The tissue sections were examined under a microscope.

Analysis of inflammatory cytokines, serum chemistry profiles, and hematology parameters. Blood was drawn from the saphenous veins of all the monkeys prior to vector administration and at 3, 6, 24, 72, and 96 hours after vector administration. Blood samples were collected into separate tubes containing either EDTA or no anticoagulant, for hematology and for determination of inflammatory cytokines and serum chemistry, respectively. Serum samples for analysis of inflammatory cytokines and serum chemistry were separated by centrifugation (4 °C, 2,500 rpm, 15 minutes), stored in a freezer at −80 °C, and thawed at the time of measurement. The levels of inflammatory cytokines (IL-6 and interferon-γ) in serum samples were measured using enzyme-linked immunosorbent assay (BioSource, Camarillo, CA). The serum chemistry parameters, which were measured with an automated chemistry analyzer AU400 (OLYMPUS, Tokyo, Japan), included AST, alanine aminotransferase, CPK, alkaline phosphatase, lactate dehydrogenase, and C-reactive protein. The hematology parameters that were determined included white blood cells, red blood cells, hemoglobin, platelets, $CD3^+$ cells, $CD4^+$ cells, $CD8^+$ cells, $CD16^+$ cells, $CD20^+$ cells, $CD29^+$ cells, and $CD69^+$ cells.

ACKNOWLEDGMENTS

The authors thank Fumiko Ono and Chieko Ohno (The Corporation for Production and Research of Laboratory Primates, Tsukuba City, Ibardki, Japan) for their help. This work was supported by grants from the Ministry of Health, Labour, and Welfare of Japan and a Grant-in-Aid for Scientific Research on Priority Areas of the Ministry of Education, Culture, Sports, Science, and Technology (MEXT) of Japan.

SUPPLEMENTARY MATERIAL

Figure S1. *In vivo* transduction efficiencies of Ad35 and Ad5 vectors in cultured cynomolgus monkey T-cell line H-SCF.

Table S1. Dosing of cynomolgus macaques with β-galactosidase-expressing Ad vectors in this study.

REFERENCES

1. Havenga, MJ, Lemckert, AA, Ophorst, OJ, van Meijer, M, Germeraad, WT, Grimbergen, J *et al.* (2002). Exploiting the natural diversity in adenovirus tropism for therapy and prevention of disease. *J Virol* **76**: 4612–4620.
2. De Jong, JC, Wermenbol, AG, Verweij-Uijterwaal, MW, Slaterus, KW, Wertheim-Van Dillen, P, Van Doornum, GJ *et al.* (1999). Adenoviruses from human immunodeficiency virus-infected individuals, including two strains that represent new candidate serotypes Ad50 and Ad51 of species B1 and D, respectively. *J Clin Microbiol* **37**: 3940–3945.
3. Wickham, TJ (2000). Targeting adenovirus. *Gene Ther* **7**: 110–114.
4. Ophorst, OJ, Radosević, K, Havenga, MJ, Pau, MG, Holterman, L, Berkhout, B *et al.* (2006). Immunogenicity and protection of a recombinant human adenovirus serotype 35-based malaria vaccine against *Plasmodium yoelii* in mice. *Infect Immun* **74**: 313–320.
5. Chirmule, N, Propert, K, Magosin, S, Qian, Y, Qian, R and Wilson, J (1999). Immune responses to adenovirus and adeno-associated virus in humans. *Gene Ther* **6**: 1574–1583.
6. Vlachaki, MT, Hernandez-Garcia, A, Ittmann, M, Chhikara, M, Aguilar, LK, Zhu, X *et al.* (2002). Impact of preimmunization on adenoviral vector expression and toxicity in a subcutaneous mouse cancer model. *Mol Ther* **6**: 342–348.
7. Muruve, DA (2004). The innate immune response to adenovirus vectors. *Hum Gene Ther* **15**: 1157–1166.
8. Koizumi, N, Kawabata, K, Sakurai, F, Watanabe, Y, Hayakawa, T and Mizuguchi, H (2006). Modified adenoviral vectors ablated for coxsackievirus-adenovirus receptor, alphav integrin, and heparan sulfate binding reduce *in vivo* tissue transduction and toxicity. *Hum Gene Ther* **17**: 264–279.
9. Koizumi, N, Yamaguchi, T, Kawabata, K, Sakurai, F, Sasaki, T, Watanabe, Y *et al.* (2007). Fiber-modified adenovirus vectors decrease liver toxicity through reduced IL-6 production. *J Immunol* **178**: 1767–1773.
10. Raper, SE, Chirmule, N, Lee, FS, Wivel, NA, Bagg, A, Gao, GP *et al.* (2003). Fatal systemic inflammatory response syndrome in a ornithine transcarbamylase deficient patient following adenoviral gene transfer. *Mol Genet Metab* **80**: 148–158.
11. Sakurai, F, Mizuguchi, H and Hayakawa, T (2003). Efficient gene transfer into human $CD34^+$ cells by an adenovirus type 35 vector. *Gene Ther* **10**: 1041–1048.
12. Sakurai, F, Mizuguchi, H, Yamaguchi, T and Hayakawa, T (2003). Characterization of *in vitro* and *in vivo* gene transfer properties of adenovirus serotype 35 vector. *Mol Ther* **8**: 813–821.
13. Seshidhar Reddy, P, Ganesh, S, Limbach, MP, Brann, T, Pinkstaff, A, Kaloss, M *et al.* (2003). Development of adenovirus serotype 35 as a gene transfer vector. *Virology* **311**: 384–393.
14. Vogels, R, Zuijdgeest, D, van Rijnsoever, R, Hartkoorn, E, Damen, I, de Béthune, MP *et al.* (2003). Replication-deficient human adenovirus type 35 vectors for gene transfer and vaccination: efficient human cell infection and bypass of preexisting adenovirus immunity. *J Virol* **77**: 8263–8271.
15. Gao, W, Robbins, PD and Gambotto, A (2003). Human adenovirus type 35: nucleotide sequence and vector development. *Gene Ther* **10**: 1941–1949.
16. Gaggar, A, Shayakhmetov, DM and Lieber, A (2003). CD46 is a cellular receptor for group B adenoviruses. *Nat Med* **9**: 1408–1412.
17. Segerman, A, Atkinson, JP, Marttila, M, Dennerquist, V, Wadell, G and Arnberg, N (2003). Adenovirus type 11 uses CD46 as a cellular receptor. *J Virol* **77**: 9183–9191.
18. Tsujimura, A, Shida, K, Kitamura, M, Nomura, M, Takeda, J, Tanaka, H *et al.* (1998). Molecular cloning of a murine homologue of membrane cofactor protein (CD46): preferential expression in testicular germ cells. *Biochem J* **330**: 163–168.
19. Hsu, EC, Sabatinos, S, Hoedemaeker, FJ, Rose, DR and Richardson, CD (1999). Use of site-specific mutagenesis and monoclonal antibodies to map regions of CD46 that interact with measles virus H protein. *Virology* **258**: 314–326.
20. Gao, GP, Yang, Y and Wilson, JM (1996). Biology of adenovirus vectors with E1 and E4 deletions for liver-directed gene therapy. *J Virol* **70**: 8934–8943.
21. Brunetti-Pierri, N, Palmer, DJ, Beaudet, AL, Carey, KD, Finegold, M and Ng, P (2004). Acute toxicity after high-dose systemic injection of helper-dependent adenoviral vectors into nonhuman primates. *Hum Gene Ther* **15**: 35–46.
22. Sakurai, F, Murakami, S, Kawabata, K, Okada, N, Yamamoto, A, Seya, T *et al.* (2006). The short consensus repeats 1 and 2, not the cytoplasmic domain, of human CD46 are crucial for infection of subgroup B adenovirus serotype 35. *J Control Release* **113**: 271–278.
23. Gaggar, A, Shayakhmetov, DM, Liszewski, MK, Atkinson, JP and Lieber, A (2005). Localization of regions in CD46 that interact with adenovirus. *J Virol* **79**: 7503–7513.
24. Fleischli, C, Verhaagh, S, Havenga, M, Sirena, D, Schaffner, W, Cattaneo, R *et al.* (2005). The distal short consensus repeats 1 and 2 of the membrane cofactor protein CD46 and their distance from the cell membrane determine productive entry of species B adenovirus serotype 35. *J Virol* **79**: 10013–10022.
25. Sakurai, F, Kawabata, K, Koizumi, N, Inoue, N, Okabe, M, Yamaguchi, T *et al.* (2006). Adenovirus serotype 35 vector-mediated transduction into human CD46-transgenic mice. *Gene Ther* **13**: 1118–1126.
26. Verhaagh, S, de Jong, E, Goudsmit, J, Lecollinet, S, Gillissen, G, de Vries, M *et al.* (2006). Human CD46-transgenic mice in studies involving replication-incompetent adenoviral type 35 vectors. *J Gen Virol* **87**: 255–265.
27. Ni, S, Bernt, K, Gaggar, A, Li, ZY, Kiem, HP and Lieber, A (2005). Evaluation of biodistribution and safety of adenovirus vectors containing group B fibers after intravenous injection into baboons. *Hum Gene Ther* **16**: 664–677.
28. Shayakhmetov, DM, Li, ZY, Ternovoi, V, Gaggar, A, Gharwan, H and Lieber, A (2003). The interaction between the fiber knob domain and the cellular attachment receptor determines the intracellular trafficking route of adenoviruses. *J Virol* **77**: 3712–3723.
29. Ichida, S, Yuzawa, Y, Okada, H, Yoshioka, K and Matsuo, S (1994). Localization of the complement regulatory proteins in the normal human kidney. *Kidney Int* **46**: 89–96.
30. Maisner, A, Zimmer, G, Liszewski, MK, Lublin, DM, Atkinson, JP and Herrler, G (1997). Membrane cofactor protein (CD46) is a basolateral protein that is not endocytosed. Importance of the tetrapeptide FTSL at the carboxyl terminus. *J Biol Chem* **272**: 20793–20799.
31. Shayakhmetov, DM, Papayannopoulou, T, Stamatoyannopoulos, G and Lieber, A (2000). Efficient gene transfer into human $CD34^+$ cells by a retargeted adenovirus vector. *J Virol* **74**: 2567–2583.
32. Stone, D, Liu, Y, Li, ZY, Tuve, S, Strauss, R and Lieber, A (2007). Comparison of adenoviruses from species B, C, e, and f after intravenous delivery. *Mol Ther* **15**: 2146–2153.
33. Nanda, A, Lynch, DM, Goudsmit, J, Lemckert, AA, Ewald, BA, Sumida, SM *et al.* (2005). Immunogenicity of recombinant fiber-chimeric adenovirus serotype 35 vector-based vaccines in mice and rhesus monkeys. *J Virol* **79**: 14161–14168.
34. Lemckert, AA, Sumida, SM, Holterman, L, Vogels, R, Truitt, DM, Lynch, DM *et al.* (2005). Immunogenicity of heterologous prime-boost regimens involving recombinant adenovirus serotype 11 (Ad11) and Ad35 vaccine vectors in the presence of anti-Ad5 immunity. *J Virol* **79**: 9694–9701.
35. Nazir, SA and Metcalf, JP (2005). Innate immune response to adenovirus. *J Investig Med* **53**: 292–304.
36. Mizuguchi, H and Hayakawa, T (2002). Enhanced antitumor effect and reduced vector dissemination with fiber-modified adenovirus vectors expressing herpes simplex virus thymidine kinase. *Cancer Gene Ther* **9**: 236–242.
37. Okada, Y, Okada, N, Mizuguchi, H, Hayakawa, T, Mayumi, T and Mizuno, N (2003). An investigation of adverse effects caused by the injection of high-dose TNFa-expressing adenovirus vector into established murine melanoma. *Gene Ther* **10**: 700–705.
38. Mizuguchi, H and Kay, MA (1998). Efficient construction of a recombinant adenovirus vector by an improved *in vitro* ligation method. *Hum Gene Ther* **9**: 2577–2583.
39. Mizuguchi, H and Kay, MA (1999). A simple method for constructing E1- and E1/E4-deleted recombinant adenoviral vectors. *Hum Gene Ther* **10**: 2013–2017.
40. Sakurai, F, Kawabata, K, Yamaguchi, T, Hayakawa, T and Mizuguchi, H (2005). Optimization of adenovirus serotype 35 vectors for efficient transduction in human hematopoietic progenitors: comparison of promoter activities. *Gene Ther* **12**: 1424–1433.
41. Maizel, JV, Jr, White, DO and Scharff, MD (1968). The polypeptides of adenovirus. I. Evidence for multiple protein components in the virion and a comparison of types 2, 7A, and 12. *Virology* **36**: 115–125.
42. Nakamura, T, Sato, K and Hamada, H (2003). Reduction of natural adenovirus tropism to the liver by both ablation of fiber-coxsackievirus and adenovirus receptor interaction and use of replaceable short fiber. *J Virol* **77**: 2512–2521.
43. Sakurai, F, Nishioka, T, Saito, H, Baba, T, Okuda, A, Matsumoto, O *et al.* (2001). Interaction between DNA-cationic liposome complexes and erythrocytes is an important factor in systemic gene transfer via the intravenous route in mice: the role of the neutral helper lipid. *Gene Ther* **8**: 677–686.

miR-122a-Regulated Expression of a Suicide Gene Prevents Hepatotoxicity Without Altering Antitumor Effects in Suicide Gene Therapy

Takayuki Suzuki[1,2], Fuminori Sakurai[1], Shin-ichiro Nakamura[3], Emi Kouyama[1], Kenji Kawabata[1], Masuo Kondoh[2], Kiyohito Yagi[2] and Hiroyuki Mizuguchi[1,4]

[1]Laboratory of Gene Transfer and Regulation, National Institute of Biomedical Innovation, Osaka, Japan; [2]Laboratory of Bio-Functional Molecular Chemistry, Graduate School of Pharmaceutical Sciences, Osaka University, Osaka, Japan; [3]Research Center of Animal Life Science, Shiga University of Medical Science, Shiga, Japan; [4]Graduate of Pharmaceutical Sciences, Osaka University, Osaka, Japan

The combined use of adenovirus (Ad) vectors expressing herpes simplex virus thymidine kinase (HSVtk) and ganciclovir (GCV) offers a potential therapeutic strategy against cancer. However, intratumorally injected Ad vectors are disseminated into the systemic circulation and efficiently transduce the liver, resulting in severe hepatotoxicity. In order to overcome this problem, an Ad vector carrying a microRNA (miRNA)-regulated expression system was developed by inserting into the 3′-untranslated region (3′-UTR) of the expression cassette four tandem copies of sequences with perfect complementarity to miR-122a, which exhibits liver-specific expression. Transgene expression from the Ad vector carrying the miR-122a target sequences was 7- to 70-fold lower in cells with high miR-122a expression as compared to expression from a conventional Ad vector. Intratumoral injection of the Ad vector containing the miR-122a target sequences resulted in a 130- to 1,500-fold reduction in hepatic transgene products (without affecting the transgene expression in the tumor) when compared with those from a conventional Ad vector. In suicide gene therapy, the inclusion of the miR-122a target sequences in the HSVtk expression cassette achieved not only significant antitumor effects, but also a dramatic reduction in HSVtk/GCV-induced hepatotoxicity. These results indicate that Ad vectors that mediate miR-122a-regulated HSVtk expression provide a safe and efficient suicide gene therapy strategy.

Received 24 April 2008; accepted 2 July 2008; published online 29 July 2008. doi:10.1038/mt.2008.159

INTRODUCTION

Among various approaches to gene therapies for cancer, suicide cancer gene therapy using the herpes simplex virus thymidine kinase (HSVtk) gene and ganciclovir (GCV) has shown some promise in preclinical and clinical studies.[1–6] The therapeutic principle of the HSVtk/GCV system consists of the transduction of the HSVtk gene in tumor cells and the conversion of nontoxic GCV to highly toxic phosphorylated GCV by HSVtk, resulting in the death of cells expressing HSVtk by inhibition of DNA replication. In addition, the antitumor effects of the HSVtk/GCV system are enhanced by a so-called bystander effect, namely, the transfer of phosphorylated GCV from HSVtk-expressing tumor cells to untransduced tumor cells through cellular gap junctions.[7,8]

Several gene delivery vehicles, including adenovirus (Ad) vectors, retrovirus vectors, and cationic lipids, have been used in HSVtk/GCV gene therapy. Among these, Ad vectors have several advantages over other viral and nonviral vectors because they can be grown to high titers and have efficient transduction activity.[9,10] In clinical studies, Ad vectors are often locally administered into tumors; however, intratumorally injected Ad vectors are systemically disseminated from the tumor, even when only small volumes of Ad vector are injected with great care.[11–13] Subsequently, Ad vectors that have leaked from a tumor primarily transduce the liver because of their high hepatic tropism, giving rise to HSVtk expression in the liver and leading on to severe hepatic damage. In order to enhance the safety and effectiveness of suicide gene therapy involving HSVtk-expressing Ad vectors, unwanted Ad vector–mediated transduction in the liver should be reduced without simultaneously reducing transgene expression in the tumor.

Recently, increasing attention has been focused on a vast post-transcriptional regulatory network mediated by microRNAs (miRNAs), which are endogenous, small, noncoding RNAs with distinct developmental and tissue-specific expression profiles.[14–20] miRNAs, which are created from long primary transcripts by several processing steps, suppress gene expression by interacting with partial complementary sequences in the 3′-untranslated region (3′-UTR) of target mRNA through association with the RNA-induced silencing complex. Recent studies have demonstrated that the insertion of miRNA target sequences into the 3′-UTR of a gene expression cassette reduced expression levels of the introduced gene, the extent of reduction being dependent on the cellular expression levels of the miRNA.[21,22] We hypothesized that insertion of sequences complementary to miR-122a,[23] which is highly expressed in the liver, into the 3′-UTR of a transgene

Correspondence: Hiroyuki Mizuguchi, Laboratory of Gene Transfer and Regulation, National Institute of Biomedical Innovation, 7-6-8, Saito Asagi, Ibaragi city, Osaka, 567-0085, Japan. E-mail: mizuguch@nibio.go.jp

expression cassette in Ad vectors would reduce hepatic transduction without affecting transgene expression in the tumor.

In this study, we demonstrate that an Ad vector carrying the miR-122a-regulated transgene expression cassette achieves efficient transduction in the tumors and reduced transgene expression in the liver after intratumoral administration. In suicide cancer gene therapy involving HSVtk-expressing Ad vectors, the miR-122a-regulated expression system not only exerted antitumor effects, but also significantly reduced the hepatotoxicity caused by Ad vector–mediated HSVtk expression.

RESULTS

Construction of an Ad vector carrying a miR-122a-regulated transgene expression system

In order to develop an Ad vector that can achieve both reduced hepatic transduction and efficient transgene expression in tumors, four tandem copies of sequences with perfect complementarity to miR-122a were inserted into the 3′-UTR of a *firefly* luciferase expression cassette in the E1-deleted region of the Ad vector genome (**Figure 1c**). miR-122a has been demonstrated to be highly expressed in the liver.[24,25] We confirmed that the use of four copies of the miR-122a target sequences achieved a more efficient reduction in *firefly* luciferase expression than the use of two copies did (data not shown). Ad vectors containing no miRNA target sequences or reverse sequences of the miR-122a target sequences were used as control vectors in this study (**Figure 1a** and **b**). The *renilla* luciferase expression cassette was inserted into the E3-deleted region to correct for the *firefly* luciferase expression levels. Conventional Ad vectors and those containing the miR-122a-regulated transgene expression system typically grew to similar extents (data not shown).

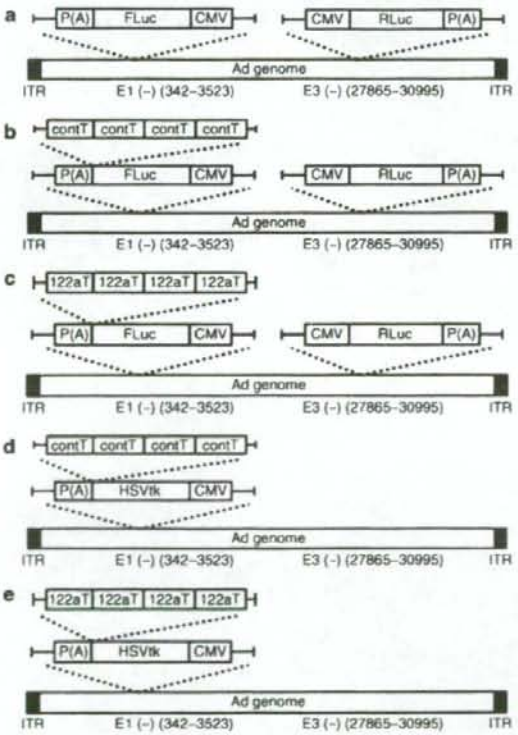

Figure 1 Schematic diagrams of adenovirus (Ad) vectors used in this study. (**a**) Ad-L, (**b**) Ad-L-controlT, (**c**) Ad-L-122aT, (**d**) Ad-tk-controlT, and (**e**) Ad-tk-122aT. A *renilla* luciferase expression cassette was inserted into the E3-deleted region to correct for *firefly* luciferase expression. CMV, cytomegalovirus promoter; HSVtk, herpes simplex virus thymidine kinase; 122aT, miR-122a target sequences; controlT, reverse sequences of miR-122a target sequences. ITR, inverted terminal repeat.

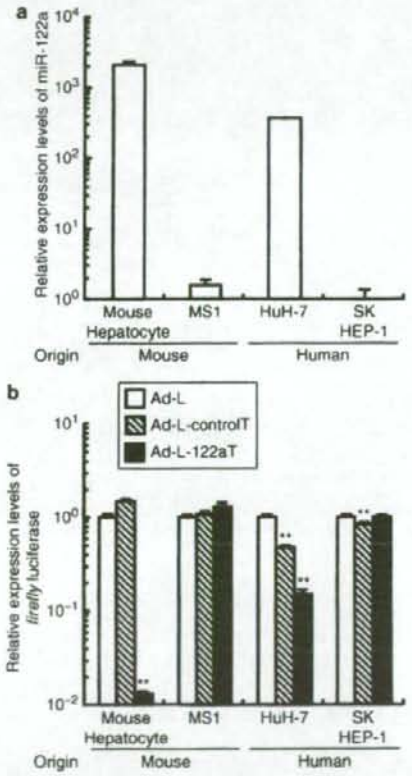

Figure 2 *In vitro firefly* luciferase expression in human and mouse cells transduced with adenovirus (Ad) vectors containing the miR-122a target sequences. (**a**) Relative miR-122a expression levels in cells as assessed by quantitative reverse transcriptase-PCR. The ratios of expression levels of miR-122a to U6 are shown as relative miR-122a expression levels. The relative miR-122a expression level in SK HEP-1 cells was normalized to 10^0. Data are presented as mean value ± S.E. ($n = 3$). (**b**) Relative *firefly* luciferase expression levels after transduction at 300 virus particles (VP)/cell. The cells were transduced with Ad vectors for 1.5 hours. After a 48-hour incubation, the cells were harvested and subjected to *firefly* and *renilla* luciferase expression analyses. *Firefly* luciferase expression was normalized to the *renilla* luciferase expression. Data are presented as mean value ± SE ($n = 3$). Significant difference, $^{**}P < 0.005$ compared with Ad-L. Similar results were obtained when the cells were transduced with the Ad vectors at 30 VP/cell (data not shown).